VYSOKÉ UČENÍ TECHNICKÉ V BRNĚ
BRNO UNIVERSITY OF TECHNOLOGY

FAKULTA STROJNÍHO INŽENÝRSTVÍ
FACULTY OF MECHANICAL ENGINEERING

ÚSTAV STROJÍRENSKÉ TECHNOLOGIE
INSTITUTE OF MANUFACTURING TECHNOLOGY

VYUŽITÍ TERMICKÉ ANALÝZY LITIN PRO PREDIKCI KVALITY ODLITKŮ NUMERICKOU SIMULACI

UTILIZATION OF THERMAL ANALYSIS FOR CASTING QUALITY PREDICTION BY MEANS OF NUMERICAL SIMULATION

DIPLOMOVÁ PRÁCE
MASTER'S THESIS

AUTOR PRÁCE — **Bc. Richard Malatin**
AUTHOR

VEDOUCÍ PRÁCE — **doc. Ing. Jaromír Roučka, CSc.**
SUPERVISOR

BRNO 2018

Abstrakt
Táto práca sa zaoberá analýzou krieviek chladnutia tvárnej liatiny a odhaluje možnosti predikcie náchylnosti na vady typu staženín z výsledkov termickej analýzy. Táto práca sa uskutočnila v prevádzkových podmienkach zlievarne, kde sa zhromaždili dáta z termickej analýzy, ktoré súviseli s odliatými vzorkami, pri kotrých sa stanovila veľkosť sťaženín. Následne sa nadobudnuté dáta vyhodnotili a hľadala sa súvislosť medzi výsledami dát termickej analýzy a vzniknutými staženinami.

Summary
This work deals with problem of analyzing cooling curves of ductile iron and discovering possibility to predict shrinkage tendency of melt from thermal analysis results. This work was executed in foundry production conditions where obtained data from thermal analysis data linked to experimental castings where amount of shrinkage was estimated. Data were analyzed and looked for correlations between acquired thermal data and shrinkage defects.

Klíčová slova
tvárna liatina, termická analýza, predikcia staženín

Keywords
ductile iron, thermal analysis, prediction of shrinkage

MALATIN, R. *Využití termické analýzy litin pro predikci kvality odlitku numerickou simulaci*. Brno: Vysoké učení technické v Brně, Fakulta strojního inženýrství, 2018. 47 s. Vedoucí doc. Ing. Jaromír Roučka, CSc.

Vyhlasujem, že som túto prácu vypracoval celkom samostatne, pod vedením doc. Ing. Jaromíra Roučku, CSc. V práci som uviedol všetky literárne pramene, zdroje a publikácie z ktorých som čerpal.

Bc. Richard Malatin

Veľmi rád by som sa poďakoval svojmu vedúcemu doc. Ing. Jaromírovi Roučkovi, CSc. za cenné pripomienky, rady a odborný dohľad pri vypracovávaní diplomovej práce.

Ďalej by som sa chcel poďakovať spoločnosti MECAS ESI s.r.o. a jej zamestnancom za podporu, zázemie a rady, ktoré mi boli poskytnuté.

V neposlednom rade by som chcel poďakovať spoločnosti VAG Hodonín, ktorá mi umožnila vykonať všetky potrebné experimenty, ktoré som pre túto prácu potreboval.

Obzvlášť špeciálne poďakovanie patrí Ing. Marekovi Blahovi zo spoločnosti VAG Hodonín, ktorý obetavo a nad rámec svojích povinností, poskytol svoj čas a úsilie, na zrealizovanie potrebných experimentov.

Zvláštne poďakovanie by som rád venoval celej mojej rodine a môjmu kocúrikovi Oliverovi, za podporu počas celého štúdia.

Bc. Richard Malatin

Contents

1 Introduction **3**

2 Literature review **4**

2.1 Shrinkage porosity 5

2.1.1 Feeding mechanisms 5

2.1.2 Morphology of shrinkage 6

2.2 Thermal analysis 7

2.3 Research review 8

3 Experimental methods **11**

3.0.1 Melt treatment 11

3.0.2 Thermal analysis 12

3.0.3 Microstructure analysis 14

3.0.4 Shrinkage evaluation 15

3.0.5 Cooling curves data smoothing 16

3.1 Preliminary experiment 18

3.1.1 Casting geometry 18

3.1.2 Experiment setup 19

3.2 1^{st} Experiment 20

3.2.1 Casting geometry 21

3.2.2 Experiment setup 22

3.3 2^{nd} Experiment 23

3.3.1 Casting Geometry 24

3.3.2 Experiment setup 25

4 Results **26**

4.1 Preliminary experiment results 26

4.2 1^{st} Experiment results 28

4.2.1 Shrinkage 29

4.2.2 Microstructure 31

4.2.3 Thermal analysis 35
4.3 2^{nd} Experiment results 36
4.3.1 Shrinkage 36
4.3.2 Microstructure 38
4.3.3 Thermal analysis 40

5 Discussion **41**

6 Conclusion **45**

1. Introduction

Production of nodular cast iron is growing every year due to its properties or advantages over lamelar cast irons. One of major advantages is ductility that spherical shape of graphite is providing and depending on matrix, highest grades with fully feritic matrix can reach over 22% elongation. Ductile iron is used in many industries like liquid distribution where pipes and fittings are made of ductile iron. In automotive industry ductile iron have many applications ranging from engine parts, suspension to steering components.

Since solidification of nodular iron is of different nature than those of lamelar iron, foundries have to deal with different problems. In nodular cast iron, shrinkage porosity is one of the biggest issues. Not always is good gating design and feeders sufficient to fight shrinkage problem and metallurgical aspect of shrinkage in ductile iron is equally important as technological aspect.

Thermal analysis is powerful tool for foundries to control their melt quality and predict imminent problems and avoid large amounts of defective castings. Thermal analysis have grat potential to predict weather prepared melt is prone to shrinkage defect or not. This is because graphite expansion have crucial effect final shrinkage porosity. With fact that graphite have larger specific heat than iron that is released during solidification, impact on cooling curves is substantial, thermal analysis have potential to predict ductile iron melt quality.

2. Literature review

Cast iron is an iron alloy which contains at least 2% carbon. Major alloying elements are carbon and silicon. Depending on cooling rate, cast irons can solidify according to meta stable $Fe-Fe_3C$ system (white) or stable Fe-C (grey), where in meta stable system, carbon an a primary phase is in carbides form and in stable system, in graphite form. Eutectic concentration is 4,3%C for metastable and 4,25%C for stable system. Depending on local cooling rate, casting can contain products of both systems. [1]

Final properties of grey cast irons depend on alloying elements, morphology of graphite and on microstructure of matrix. Graphite can grow in lamellar (FG), vermicular (CG) or nodular shape (SG). Matrix can be feritic, feritic-perlitic, perlitic or bainitic (or austenitic after alloying). [1]

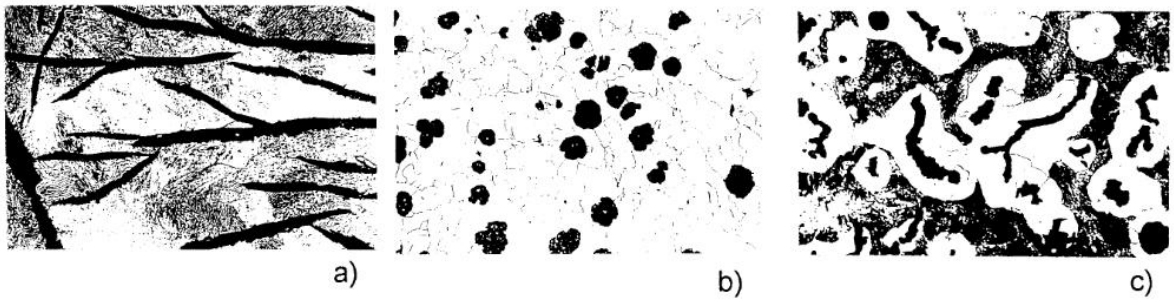

Figure 2.1: Types of graphitr: a - Lamelar, b - Nodular, c - Compacted [1]

Graphite shape is crucial not only for final mechanical properties but also castability, thermal conductivity, vibration dumping, etc. While flake graphite will give lower mechanical properties (sharp flakes acts as stress concetrators), thermal conductivity, castability (due to nature of solidification and graphitic expansion) and dampening properties are better than nodular graphite form. Nodular graphite have great influence on ductility hence name ductile iron. Vermicular graphite properties are on half way between lamellar and nodular morphology. Graphite morphology is controlled via modification using magnesium. Graphite shape will determine range of mechanical properties but final properties are given by matrix microstructure. For lamellar graphite range of tensile strength is 150 - 350 MPa and nodular irons 400 up to 800 MPa. Final matrix microstructure is result

of local cooling rate and alloying elements.
[2] [1]

2.1. Shrinkage porosity

Every material which is cooling down is accompanied with volume decrease. So certain volume of metal that is poured into mold after solidification and cooling to room temperature will occupy less volume. Shrinkage process can be divided into three parts. First is shrinkage during liquid state. At this stage contraction of liquid volume produce no problems since feeding in liquid state is almost effortless. Second stage of shrinkage is contraction during transformation from liquid to solid state. Foundation to this contraction is that solid occupy less volume due to atom are now aligned in organized way (lattice). I this stage, move of solid or liquid is necessary to compensate for contractions. This is stage where actual shrinkage defect in castings are created. Third stage of shrinkage is contraction in solid state. Contraction of unrestrained solid is linear process however in case of casting which are shrinking in rigid molds can cause that final dimensions are slightly larger than expected. [5] [3]

Solidification of a casting is done by gradual spread of solid, usually in form of growing dendrites. This growing structure will later act as a obstacle and at some point move of mass will be eventually ceased. There are five mechanism of feeding mechanism of solidifying alloy. [5]

2.1.1. Feeding mechanisms

Liquid feeding This is most free form of feeding and its main mechanism of feeders to compensate for solidifying casting. This type of feeding is most effective for skin freezing alloys, in fact for them is it only mechanism of feeding. It occurs before and at early stages of solidification

Mass feeding is movement solidified parts in residual liquid present mainly in larger cross section areas as the solidified particles can freely move in liquid. This type of feeding ends when solidified metal create coherent network.

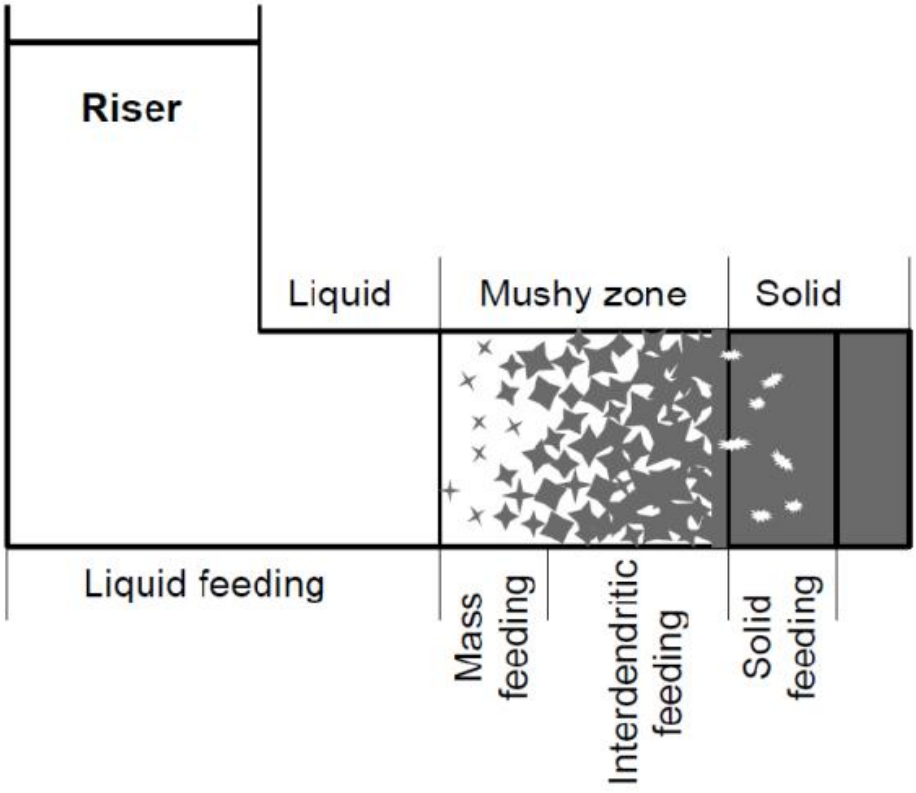

Figure 2.2: Feeding mechanism. [4]

Interdendritic feeding This type of feeding when coherent network of solidified alloy is created. At this stages liquid travel between space between dendrites.

Solid feeding At latest stages of solidification, solid feeding through plastic and elastic deformation is only option to compensate.

Burst feeding When a solidified network collapse and suddenly move larger volume of mass, this is called burst feeding. This can happen at interdendritic feeding or solid feeding stage.
[5]

2.1.2. Morphology of shrinkage

Outer Sunk are surface defects. When casting skin is solidified, melt inside shrinks further and no feeding is available, shrinking will cause negative pressure inside the cavity. If the pressure difference between atmospheric and inside casting is too large, material is pulled inwards creating outer sunk to compensate for needed material inside.

Macro shrinkage are located inside castings near hot spots. Macro shrinkage is developed at early stages of solidification and pressure difference is not sufficient to pull material inside creating outer sunk.

Micro shrinkage are smaller cavities located at hot spots. This type of shrinkage is developed at latest stages of solidification. Micro shrinkage is more metallurgical problem than technological unlike outer sunk and macroshrinkage. Micro shrinkage is usually created by insufficient graphite expansion.
[6]

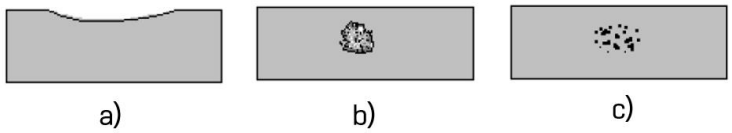

Figure 2.3: Morphology of shrinkage defects. a)Outer sunk, b)Macro shrinkage, c)Micro shrinkage [6]

2.2. Thermal analysis

Thermal analysis is tool for analyzing temperature change over time in cooling material. It is used mainly for cast irons and aluminum alloys. Thermal analysis can predict composition, dendrite arm spacing eutectic morphology, grain refinement and many more using computer analysis. [3] [7]

Simplest thermal analysis uses one thermocouple inside small test mold. Metal is poured inside cup and thermocouple is measuring temperature. The shape of cooling curve is determined by balance between the latent heat releasing during solidification and heat lost to surroundings. Shape and volume have significant effect on cooling curves as well as pouring temperature. [3] [7]

Basic and most useful information form thermal analysis for cast irons is estimation of chemical composition more precisely estimation of carbon equivalent. Since all cast irons contain considerable amount of silicon, eutectic temperature differs from those of

stable iron-carbon diagram. With system with multiple cups with one of them contains tellurium for white solidification and another tellurium with sulfur are used to estimate magnesium concentrations. [3] [7]

Another application of single thermal analysis cup is to predict eutectic structure. This is done with comparing measured eutectic temperatue with theoretical stable and metastable temperature. If start and aend of eutectic solidification is abovce metastable temperatures, melt solidified acording to stable (gray) system. If start of solidification is under metastable temperature, there is risk of chills. If temperature of end of solidification is under metastable temperature, this means risk of inverse chills. Degree of inoculation can be estimated by comparing samples with and without inoculation. [3] [7]

Prediction of graphite shape can be done from shape of cooling curve. Different shape of graphite have different surface area than flake graphite hence different heat transfer which affects cooling curve especially at the end of solidification. [3] [7]

2.3. Research review

Research for this work will eventually lead us to two kinds of problematic. First, it's understanding of shrinkage defects creation in ductile irons. Mechanism of macro and micro shrinkage creation is understood and in depth general explanation provided Campbell [5] with fact that graphite expansion plays key role in cast irons but understanding of individual variables is often problematic. Most of works concentrate on various parameters like chemical composition, recalescence [8], inoculation, feeding designs [9] etc. and tries correlates it with shrinkage volume.

Second kind of problematic is about thermal analysis itself. Understanding what kind of information cooling curves and its derivations are hiding and how it can be read. Simple information like, temperatures, undercooling, recalescence, etc. are well documented and easily extracted from cooling curve. Many authors agreed that, thermal analysis contains far more information than foundries usually benefits from.

Whilst reasonable number of articles on these topics can be found, researches aimed purposely on using thermal analysis for shrinkage prediction in ductile irons (or any particular alloy) castings are scarcer.

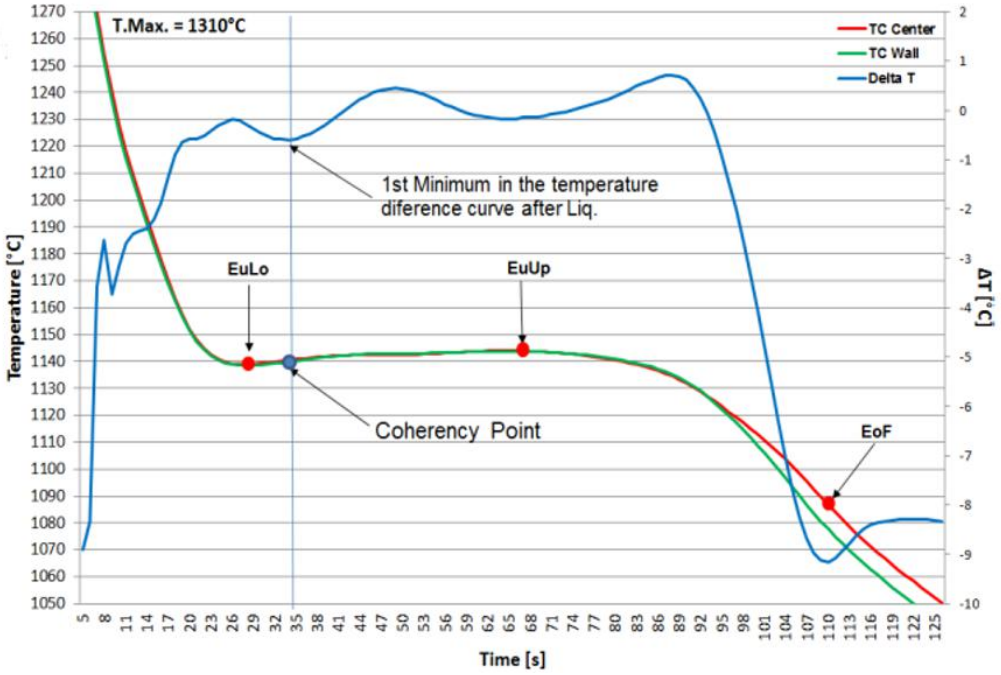

Figure 2.4: Dendrite coherency point estimated in cast iron cooling curve [10]

Vitor Emanuels dissertation thesis [10] is extensive work that covers basic theories of ductile iron solidification, thermal analysis application and interpretation, cooling curves and many more. Work is well founded with lots of experiments and data. One of interesting things that this work investigated is dendrite coherency point (DCP) for ductile iron, as author stated, no experiments for determination of DCP for ductile iron were done previously, just for aluminum alloys. Based on multiple theories, he performed experiments and described how to determine DCP for ductile iron for different solidification morphology. Hence DCP mark point after no mass feeding is possible, it should be interesting at least to investigate if it has any practical meaning in our experimentation since author didn't correlated DCP with measured shrinkage. Author did experiments where he correlated shrinkage with different carbon concentrations but in our case we will work primarily with one alloy so we can lever out this variable.

David Sparkman from company MeltLab Systems is using very different approach. Most of today thermal analysis companies extracts data from thermal analysis from cooling curve itself, its first derivative and rarely second derivative. David Sparkman is using up to fifth derivatives and information he receives is not presented as temperature or time but rather a shape itself or trends. He states that creation of shrink is endothermic process and with enough precision this is cached by thermal analysis. However, this method requires precise and fine-tuned thermal analysis device that is capable capturing enough noise free data to be able to make these higher derivatives. With that being said, smoothing these derivatives is another difficulty and David Sparkman obviously didn't reveal particular method how to do this correctly. This work tested a proposed shrinkage predictor based on thermal analysis data and was tested by experiments in three different foundries. Authors prepared an experimental casting where shrinkage volume was estimated and compared with thermal analysis data. Authors made experiments in quite a large number and used statistical methods to prove data validity. However no clear conclusions on how well predictor performed. This work is most useful for us for now, could be used as a leash for this work, experiments will be done in very similar nature.

Bradley [11] tested a proposed shrinkage predictor based on thermal analysis data and was tested by experiments in three different foundries. Authors prepared an experimental casting where shrinkage volume was estimated and compared with thermal analysis data. Authors made experiments in quite a large number and used statistical methods to prove data validity. However no clear conclusions on how well predictor performed. This work is most useful for us for now, could be used as a leash for this work, experiments will be done in very similar nature.

3. Experimental methods

Experiments will be performed at foundry VAG Hodonín a.s. which is company for producing valves, fittings and other parts for water distribution. Foundry Hodonín disposes with green sand automated production link and hand molding station for larger castings using aslo green sand technology. For cores they are using silica sand bonded by CO2 water glass . Production casting weight ranges from kilos to tens of kilos. Depending on casting different sizes of flasks are used. .

3.0.1. Melt treatment

Melt is prepared on 4 ton electric induction furnaces. Modification is done by sandwich method in 800 kg crucible right after tapping. Inooculation is carried out depending weather is casting process happening at hand molding station or automated molding link. For hand molding station is used ladle inoculation while transferring melt from sandwich crucible to smaller pouring crucible. At automated molding line, in-stream inoculation is used. Amount of inoculation depends on casting size and design. Different inoculators are used at hand molding station than at automated link. Inoculator types and composition:

Melt treatment aditions chemical composition:

Name	Purpose	%Si	%Ca	%Al	%Zr	Grading [mm]
VP216	Ladle inoculation	68-73	0.3-1.5	3.2-4.5	-	0.6-3.0
Zircinoc	In-stream inoculation	73-78	2.0-2.5	1.0-1.5	1.3-1.8	0.2-0.7
		%Si	%Mg	%RE	%Ca	%Al
Elmag9510	Modification	44-48	8.5-9.5	0.8-1.2	2.5-3.5	max 1.0

Figure 3.1: List of used inoculators and modification additions

All casted specimens in this work are marked by this system:

1. number	**2. number**	**letter**
Pouring session	Specimen characterization	Complementary Letter

Pouring session - is characterized with its melt origin therefore base metal have same chemistry. This number is common for every experiment done in this work so there will be no two different specimens with same number.

Specimen characterization - is second number indicating particular tested variable. Each experiment have different specification for numbers.

Complementary letter - third position is for description of sample origin. Weather its from thermal analysis (sign T) or if two specimens at the same time are poured (A/B), this position can be also left blank.

3.0.2. Thermal analysis

The foundry is using NovaCast ATAS thermal analysis system for melt quality control for grey and ductile iron. ATAS system is based on temperature measurements made using Quik-Cup test cups produced by Electro-Nite. Foundry Hodonín is using standart cups witjout inoculant nor Tellurium (QC 4010). Thermocopule is type K and analogue signal is transformed to digital by Datascan 7220/7221 A/D-converter. [12]

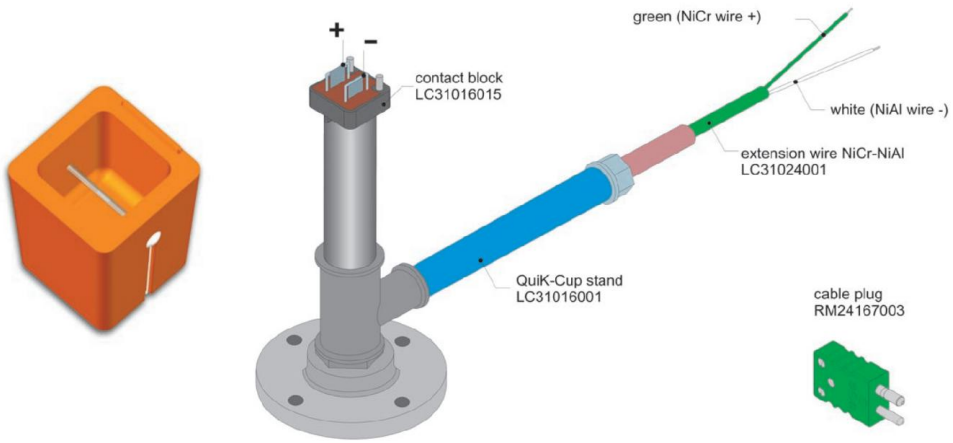

Figure 3.2: Hereaus Elektronite thermal analysis equipment [13]

ATAS thermal analysis is using cooling curve and 1^{st} derivation of cooling curve to control melt quality. System is scanning with frequency of 1 Hz and unfortunately only temperature data are able to extract from program.

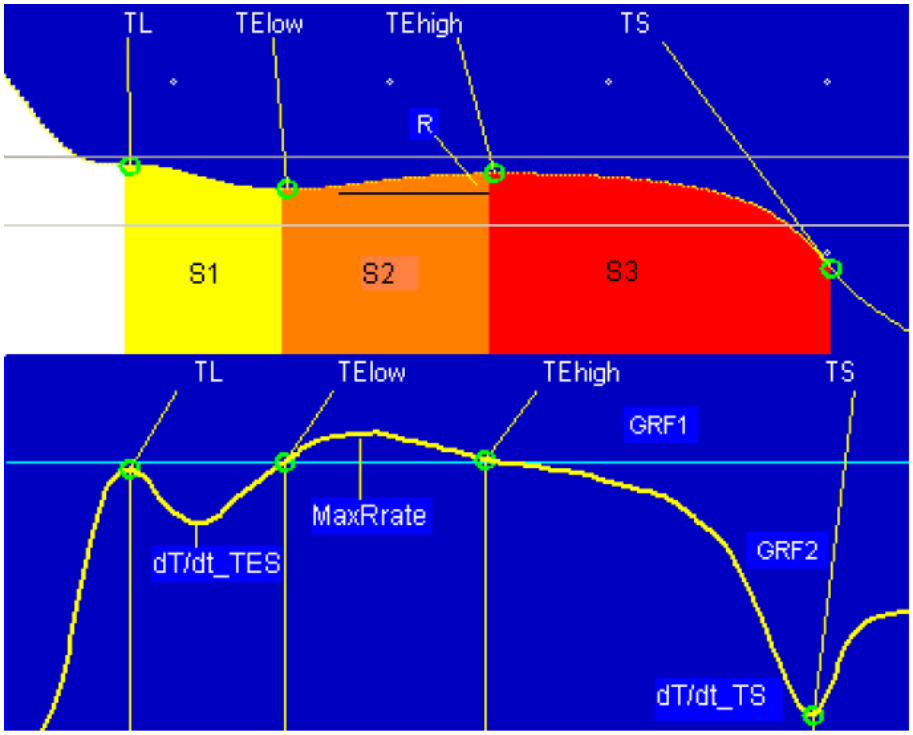

Figure 3.3: ATAS cooling curve and its derivation with marked parameters..

ATAS is gathering and analyzing following information from cooling curves and it's derivatives:

Parameter	Unit	Description
TL	[°C]	Temperature at liquidus measured as first arrest temperature. For eutectic temperature is TL same as TElow.
TES	[°C]	Temperature of start of eutectic freezing. Defined as point where derivative has minimum between TL and TElow.
dT/dt TES	[°C·s^{-1}]	Value of first derivation at TES temperature
TElow	[°C]	Lowest eutectic temperature
TEhigh	[°C]	Highest eutectic temperature
R	[°C]	Recalescence, TEhigh - TElow
TS	[°C]	Temperature at solidus. The lowest value of negative peak of derivation curve at end of solidification.
dT/dt TS	[°C·s^{-1}]	Value of first derivation at TS temperature
GRF 1		Graphite factor 1
GRF 2	[°]	Graphite factor 2
GRF 3	[°]	Graphite factor 3
S1, S2, S3	[-]	Percent surface area between TL-TElow, TElow-TEhigh, TEhigh-TS

Foundry is adding inoculant to testing cups to compensate for later added inoculation. For actual actual cooling curves from casting, thermal probes are needed but their usage in production either is very complicated or not possible at all. The way foundry works thermal analysis is bound to pretapping, premodification and after modification analysis.

In later stages thermal analysis, thermal analysis is not possible.

Measuring temperature field in castings was done with type S thermocopules (PtRh-Pt) covered in ceramic tube. Placement of thermocopules will be described in detail in experiment that they were used in. This method provided us with slightly better data density, about 3 readings per second.

3.0.3. Microstructure analysis

Samples from casting trials as well as thermal analysis samples were used also for microstructure evaluation. In both cases, samples will be extracted from thermal center region of test castings. Graphite shape and nodule count will be main observation since from microstructure analysis are these two most important factors in terms of shrinkage defects. Samples were also etched to observe ferrite to pearlite ratio and if present, carbides.

Castings were always sectioned using bandsaw and abrasive wheel under fluid cooling to prevent change of structure. Cutted samples were mounted into epoxy using hot mounting press mashine. Grinding and polishing was mechanized and done according to folowing procedure:

Step	Description	Time [min]
Grinding	Grinding disc 240 mesh	4
	Wet Grinding paper 800 mesh	4
	Wet Grinding paper 1200 mesh	4
Polishing	9 µm polishing suspension	5
	3 µm polishing suspension	5
	1 µm polishing suspension	5

After every grinding step, samples were cleaned under stream of water, polishing steps were alternating with ethanol cleaning with hot air drying. Etching was done by Nital solution.

Structure observation was done on Microscope Olympus GX71 with digital camera DP11. All images that were evaluated were done with 100x magnification.

Evaluation of graphite shape and nodule count will be done according to norm EN ISO 945-1:2008(E). For image analysis, freeware program ImageJ was used.

3.0.4. Shrinkage evaluation

Measuring shrinkage cavity was done by several methods. Before sectioning of castings, non destructive methods were used, such as double weightening or X-ray.

Double weightening is method based on Archimedes law and it is used to calculate density. Sample is weighted in air and than is immersed into container with water placed on scales. Scale will show weight of displaced water which can be used to calculate volume of immersed sample. In our case, we expect that our samples will contain shrinkage defects in different amount hence apparent density is estimated instead of true density. Samples with more shrinkage defects will produce apparent density.

Figure 3.4: Double weightening setup.

X-ray scanning was done on YXLON Smart 300. Test casting were surrounded by lead sheet metals to prevent scattering of x-rays. Castings were scanned separately.

After non destructive methods of shrinkage estimation, test castings were cutted in half throught their thermal center for visual observation. Volume of large shrinkage cavities were estimated by pouring a fine sand into cavities and then measuring sand volume.

3.0.5. Cooling curves data smoothing

Data gained from ATAS and thermal couples reading needs to be smoothed in order to get better results of its derivatives. As smoothing tool was used set VBA (Visual Basic for Application) macros for Excel. This function can perform number of smoothing methods of exploratory data analysis.

This smoothing function includes following data smoothing parameters:

1, 2, 3, 4, ... Perform a median smooth with the given window size. For medians of three, smooth the two end values using Tukey's extrapolation method. Of course, no smoothing is done for window sizes of 0 and 1, but these sizes are accepted as valid commands anyway.

R When a median smooth is immediately followed by an "R" (repeat) command, then continue to apply the median smooth until no more changes occur.

S "Split" the sequence. This process dissects the sequence into shorter subsequences at all places where two successive values are identical, applies a 3R smooth to each subsequence, reassembles them, and polishes the result with a 3 smooth.

H "Hann" the sequence. This is convolution with a symmetrical kernel having weights (1/4, 1/2, 1/4). That is, each value x[i] is replaced by x[i-1]/4 + x[i]/2 + x[i+1]/4. The end values are not changed.

, "Re-roughing". At the first appearance of a comma, the smoothed sequence will be saved, to be replaced (temporarily) by its "rough", which is the series of residuals (differences between the original and smoothed values). Until the next appearance

of a comma, the commands will be applied to the rough. Another comma (or the end of the commands) will cause the original smooth to be added back to the smoothed rough. This process can be repeated as many times as desired for repeated re-roughing.

[14]

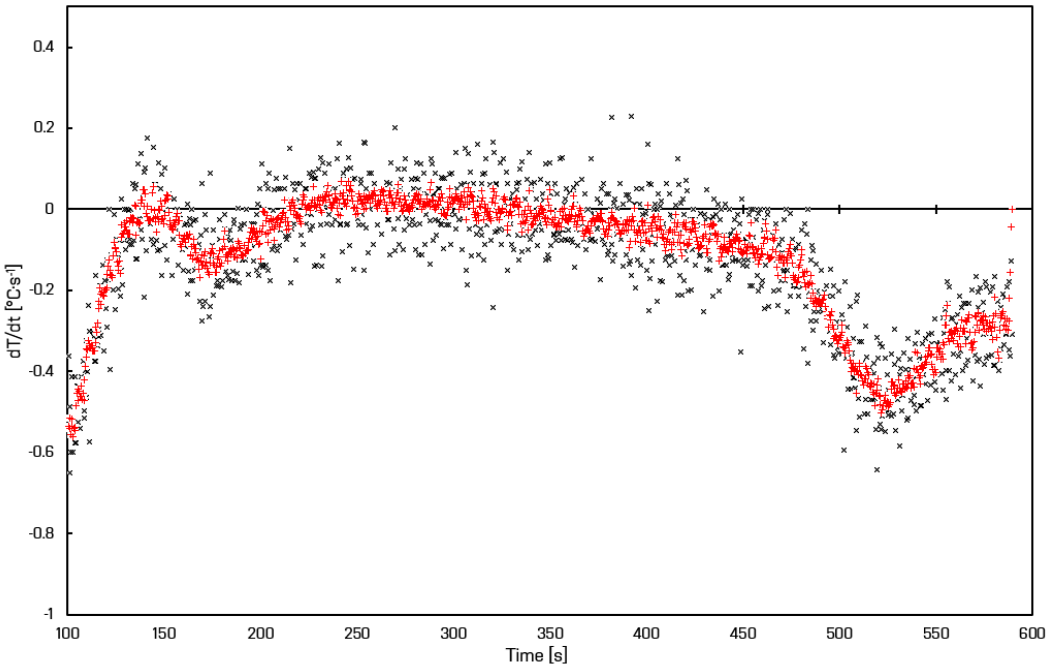

Figure 3.5: Example of data smooothing. ×- original data, + - smoothed data

I our case final parameter which was used to smooth data was "**3RSSH, 4253H, 3RSSH, 4253H**".

With faster data readings and more precise measurement, it is possible to go for higher derivatives of cooling curves. In our conditions, only 1^{st} derivative was possible to obtain.

3.1. Preliminary experiment

Preliminary experiment objectives are:

- Testing various casting geometry
- Revealing possible future issues
- Getting familiar with foundry conditions
- Preparing specimens for evaluation

Marking of preliminary test casting is done differently because these samples will not be part of thermal analysis experiments and only used as starting point in casting design.

3.1.1. Casting geometry

First type of specimen is box type casting copied from Bradleys work [11]. This design could be a problem because flat surfaces tend to depress while solidifying and this could make impact on observable shrinkage since volume of casting has decreased. In contrary to Bradleys experimental piece, second type of specimen is designed. A round cylindrical casting that should be more resistant to surface sink defects. Both of designs will be tested and after preliminary tests, one design will be choosed for next experiments.

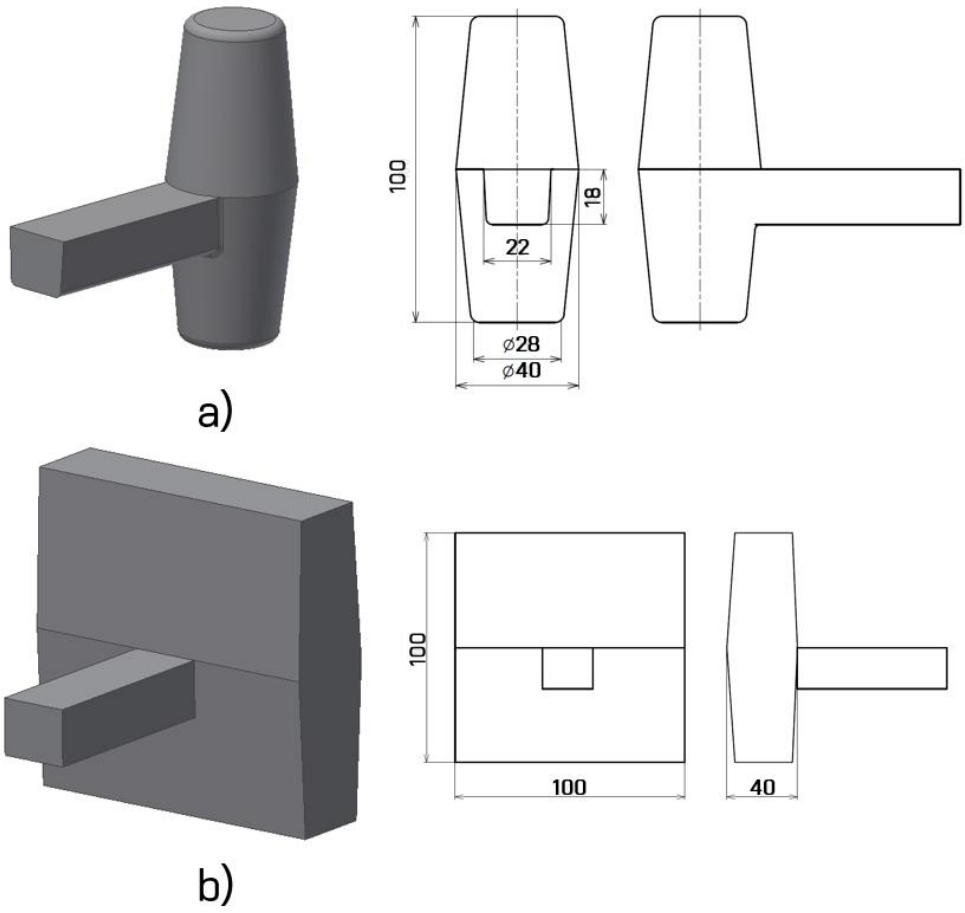

Figure 3.6: Experimental castings. a) cylinder casting, b) block casting.

3.1.2. Experiment setup

The preliminary experiment will be performed as follows: before melt in induction furnace is ready for tapping first thermal analysis is performed, this is just for chemical composition control and it has no practical use for this work. Then melt is tapped into 800 kg sandwich treatment crucible. Melt is treated with modification agent in 0,8% weight amount. After this another thermal analysis is performed to confirm successful modification. Specimens will be attached to gating system in actual production casting. Specimens will be molded in several casting which will be poured in one session. In this case, we will get different pouring temperatures, residual magnesium content and inoculation fading effect. This should produce wide range of shrinkage and test if choosed test castings are suitable for further testing.

Alloy:	GJS 400-15
Mold:	Green sand
Type of molding:	Hand molding
Innoculation:	Ladle; 0,65 wt.%
Modification:	0,8 wt.%

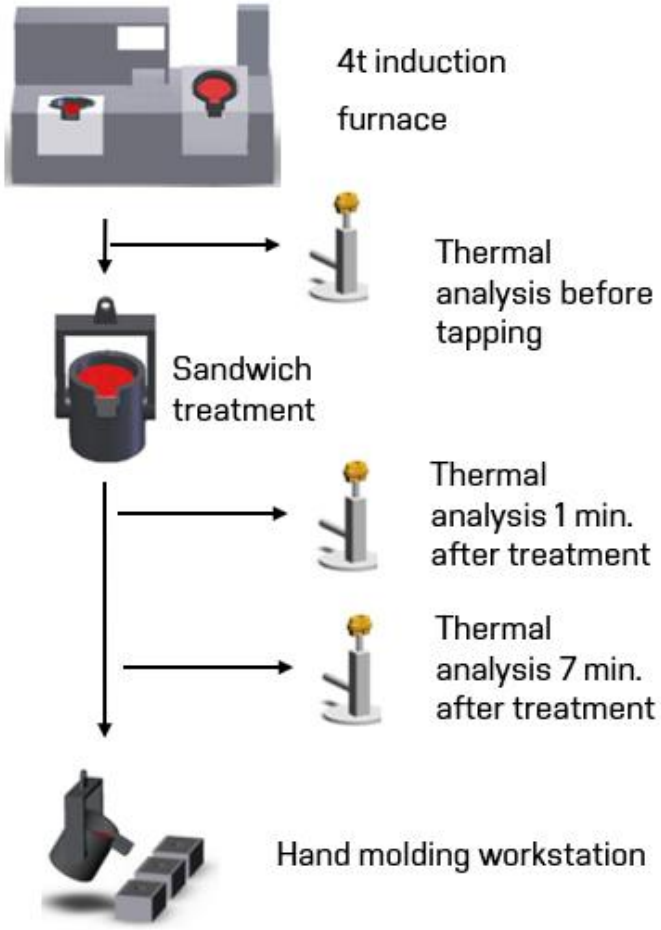

Figure 3.7: Scheme of preliminary experiment

3.2. 1^{st} Experiment

Objectives of this experiment are:

- Test influence of inoculation amount on shrinkage defects
- Gather data from ATAS thermal analysis and correlate with shrinkage
- Evaluate effect on graphite shape and amount

Marking of test castings consist of two numbers and one letter are done according to this scheme:

X	Y	Letter
	Inoculation flow	
Pouring session	1 - 2,4 g/s 2 - 4,4 g/s 3 - 6,4 g/s	A/B/T

Example: Specimen 21A means it was poured in second session with inoculant flow of 2,4 g·s^{-1} and it's casting "A" from casted pair.

3.2.1. Casting geometry

Geometry for this experiment is as cylindrical casting from preliminary tests. This model was attached to gating system on model board (Fig. 3.8). This way every casting has two identical specimens which in their markings differentiate by letter A and B. This was done to have a control specimen for shrinkage evaluation.

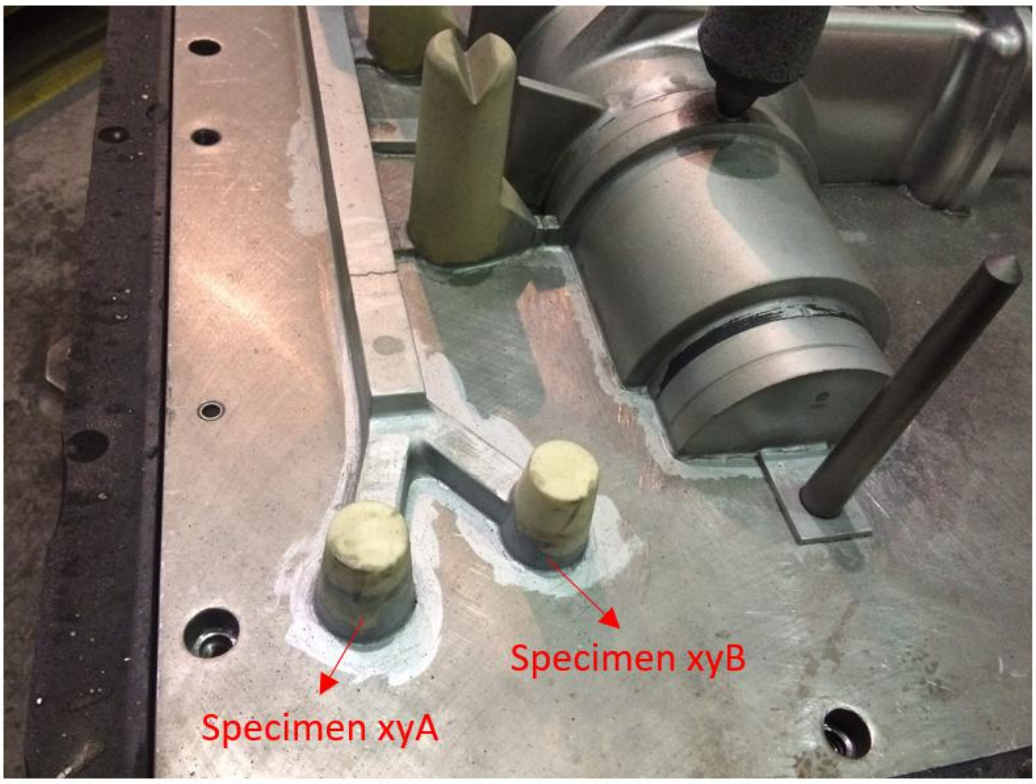

Figure 3.8: Two test castings attached to the end of gating system of production casting.

3.2.2. Experiment setup

After tapping, melt will be treated in 800kg sandwich crucible, after this melt is poured into 400kg crucible which is going to pouring line and this is point where time is measured from. From this crucible are taken samples for thermal analysis. At pouring line, temperature of melt is recorded. Between each pouring time is recorded as well. This process is repeated 3 times. After pouring, test castings will be separated from castings. Samples from thermal analysis will be kept as well.

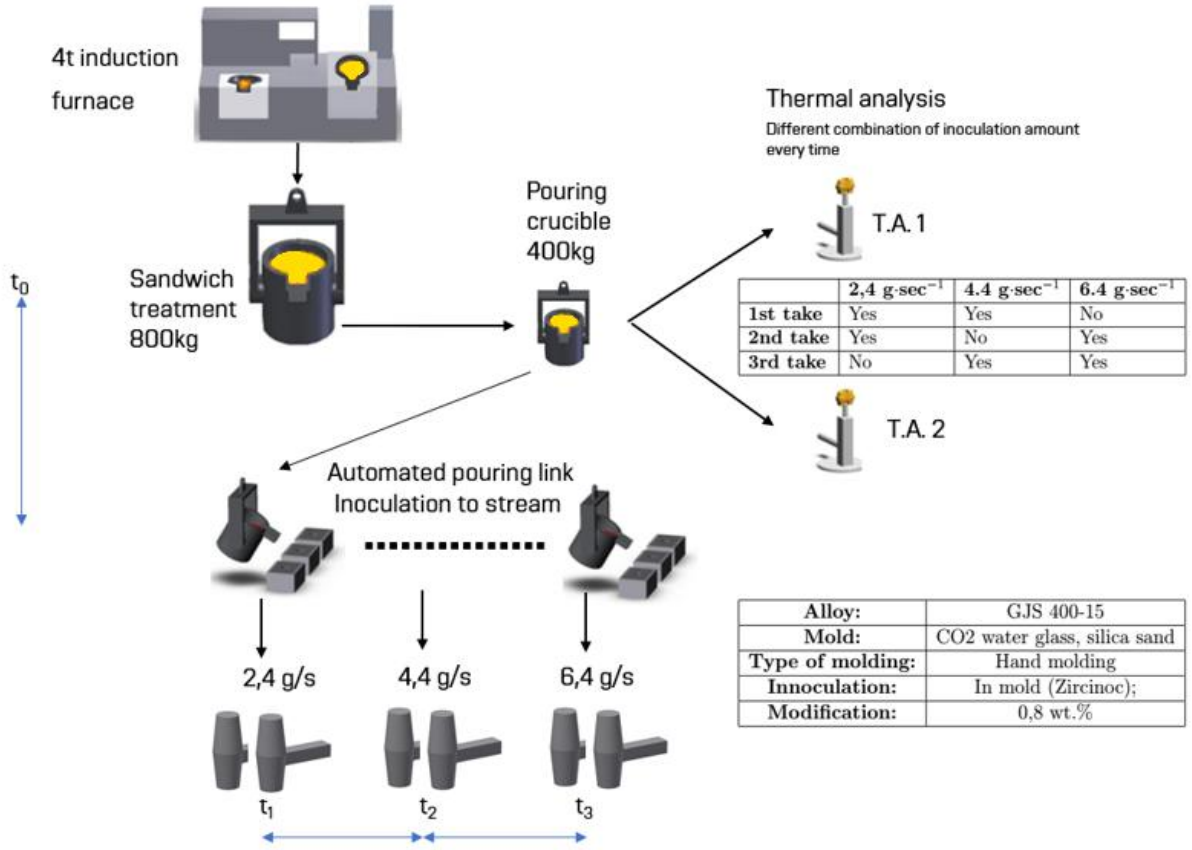

	2,4 g·sec^{-1}	4.4 g·sec^{-1}	6.4 g·sec^{-1}
1st take	Yes	Yes	No
2nd take	Yes	No	Yes
3rd take	No	Yes	Yes

Alloy:	GJS 400-15
Mold:	CO2 water glass, silica sand
Type of molding:	Hand molding
Innoculation:	In mold (Zircinoc);
Modification:	0,8 wt.%

Figure 3.9: Scheme of 1^{st} experiment

Three different inoculation amounts settings will be tested. Depending on casting size and wall thicknesses, foundry uses different amounts of inoculation flows. In our case and casting that specimens are connected to, standart rate of inoculation is 4,4 grams per second. In our testing, we also use 2,4 and 6,5 grams per second. Test casting is pair of cylinders to have control specimen for shrinkage evaluation. Thermal analysis cups will be containing corresponding amount of inoculant. Since there are only two testing cups

available for each pouring session, total of 3 pouring sessions will be performed to ensure enough data for each inoculation amount tested. In one pouring session, three castings with different inoculation rate will be poured right after each other to help keep even pouring temperature.

3.3. 2^{nd} Experiment

- Test influence of inoculation amount on shrinkage defects
- Isolate variable of inoculation completely
- Create cooling curves and its derivatives and estimate basic thermal analysis parameters
- Evaluate effect on graphite shape and amount and compare with cooling curves

Marking of castings:

X	**Y**	**Letter**
Pouring session	Inoculation amount: 0 - no inoculation 1 - 0,2 wt.% 4 - 1,0 wt.%	none

Second experiment will be done in separate flask and will not be part of production casting. This allow to use thermo couples for precise measurement of cooling curves. Each cylinder will contain different amount of inoculator which will be placed inside each gate in different amounts. This setup eliminates problem of different chemical composition and pouring temperature and truly separated influence of inoculation amount from other variables. This setup will be formed using resin bonded sand to ensure homogeneous rigidity which could be problem in hand molded green sand molds. Variation to this setup is test of different sizes of gates with constant inoculation amounts.

3.3.1. Casting Geometry

Geometry of this test casting was changed opposed to previous test castings. Volume is enlarged and gate cross section is smaller. This should help promote shrinkage defects. This casting will consist three cylinders connected to common raiser. Gates are connected laterally to to ensure good mixing of inoculant in melt. In each cylinder will be established a thermal couple placed in thermal center of cylinder.

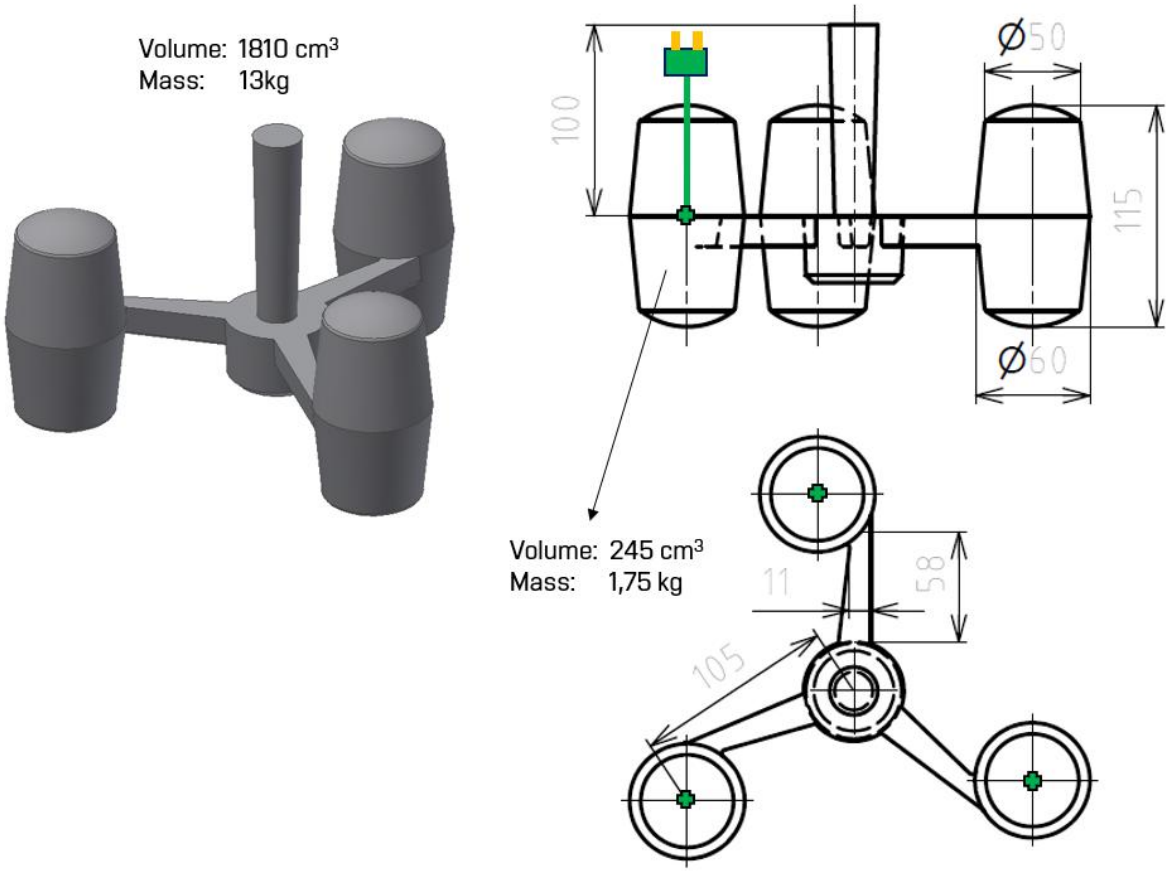

Figure 3.10: Dimensions of 2^{nd} experiment casting.

3.3.2. Experiment setup

After tapping melt will be treated for modification and poured into 400kg transferring crucible. Before is melt inoculated for hand molding station, par of non inoculated metal was poured to smaller crucible dedicated to our experiment. This non inoculated melt was poured into our separate mold.

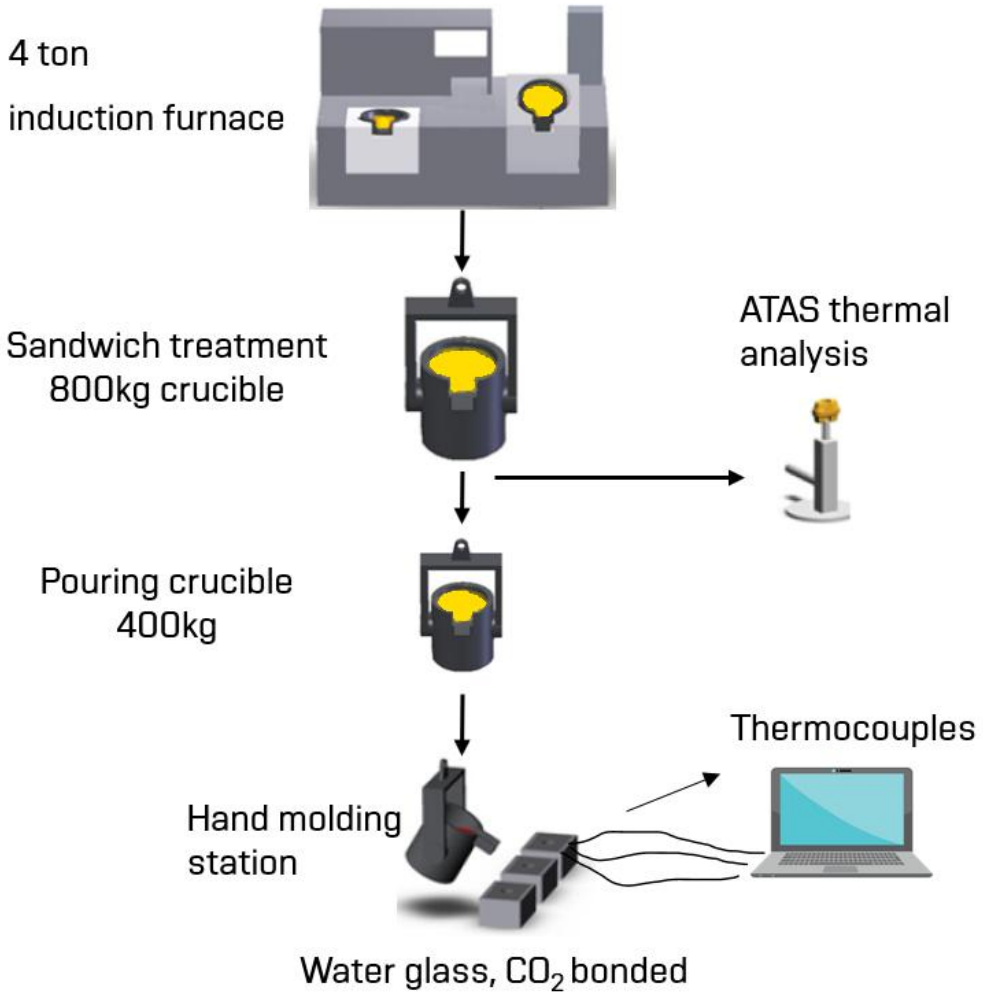

Figure 3.11: Scheme of 2^{nd} experiment.

4. Results

4.1. Preliminary experiment results

Preliminary test of castings showed that specimens produced various amounts of shrinkage defects from sound castings to macro shrinkage. Box type castings and thermal analysis samples suffered from surface sink defects. Both cylinder and box type casting showed similar volumes of shrinkage defects. Pouring temperature was not recorded since foundry uses temperature from last thermal analysis. From modification treatment to last poured casting elapsed considerable amount of time so fading of magnesium and inoculator with pouring temperature varied substantially. Exact times of pouring and between pourings were not recorded.

Base metal composition:

Casting session	**C.E.** [%]	**C** [%]	**Si** [%]	**Mn** [%]	**P** [%]	**S** [%]	**Cr** [%]	**Mg** [%]	**Cu** [%]	**Al** [%]	**Sn** [%]	**Ni** [%]
0	4,49	3,83	2,74	0,35	0,038	0,013	0,047	0,064	0,037	0,019	0,005	0,02

Figure 4.1: Left - Box casting, Right - Cylinder casting

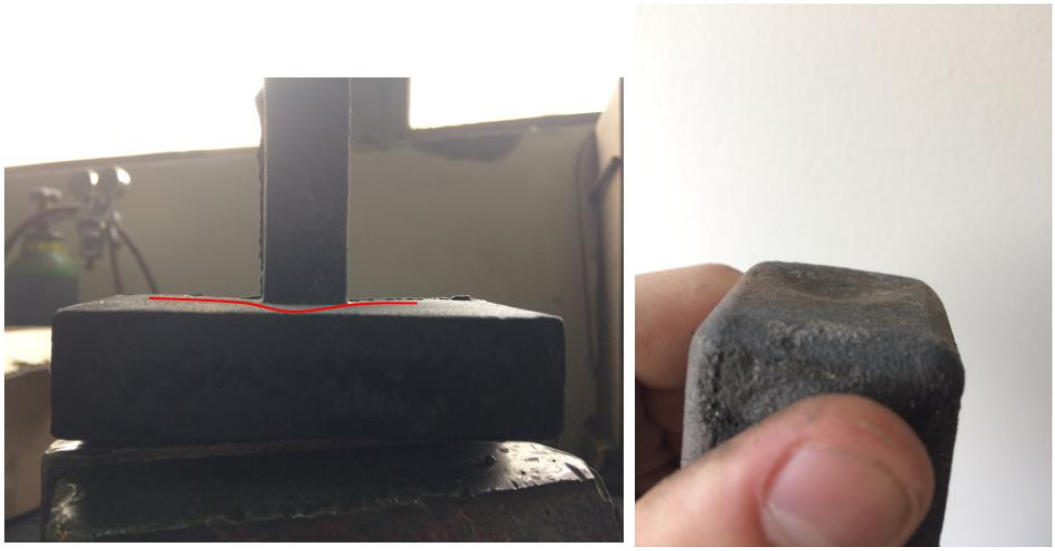

Figure 4.2: Surface sink defects.

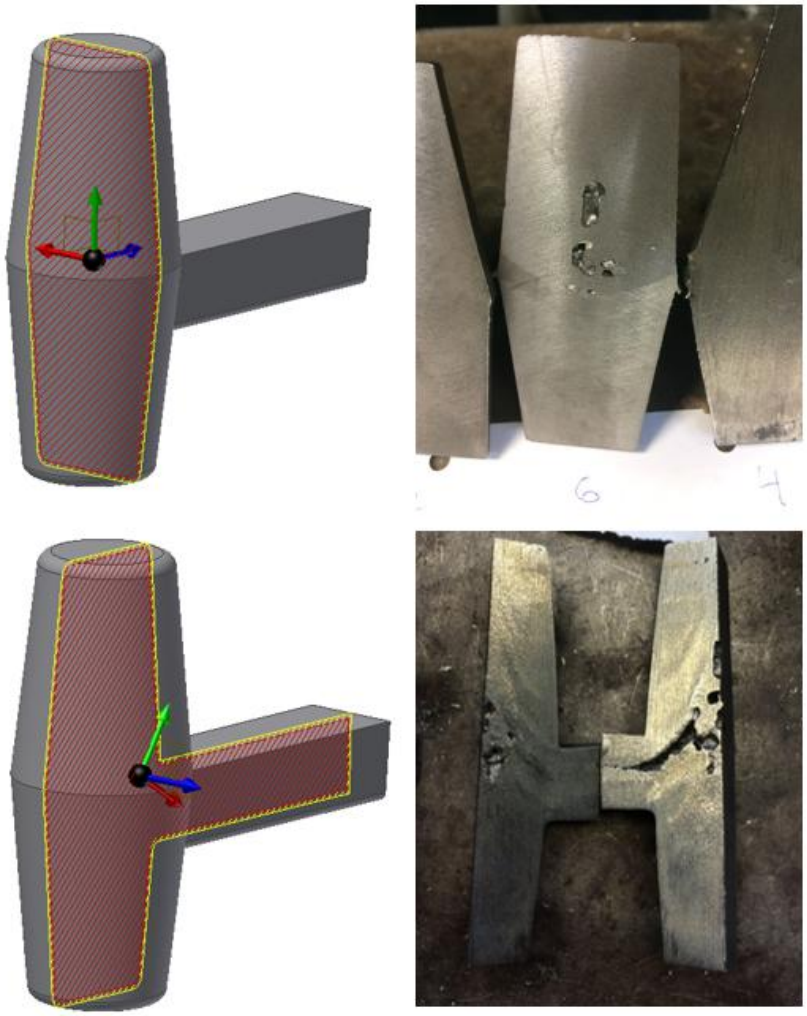

Figure 4.3: Different sectioning planes on the same sample.

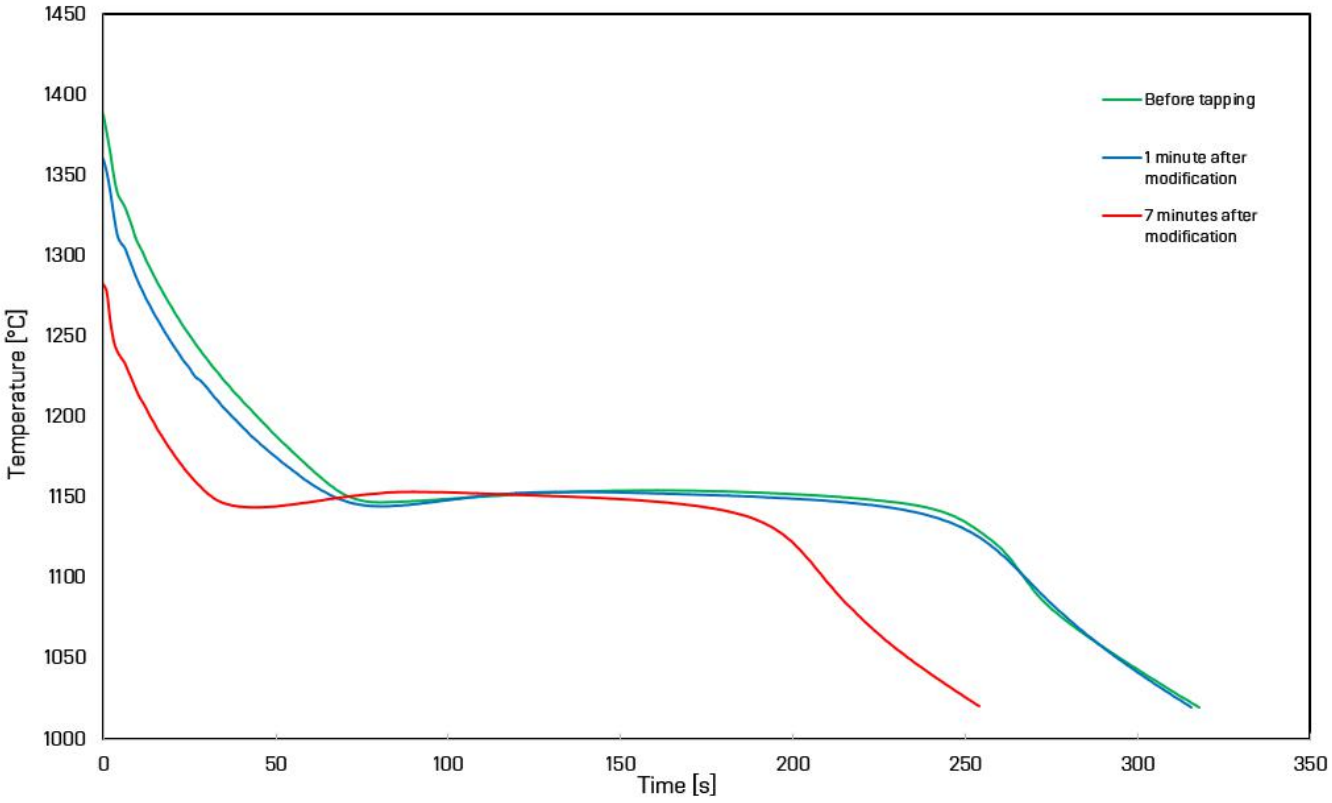

Figure 4.4: ATAS Cooling curves from preliminary testing

	ACEL	TL	TES	TElow	TEhigh	R	MaxRrate	S1	S2	S3	GRF1	GRF2	GRF3	dTdtTS	TS
Before tapping	4.239	1147.33	1147.38	1147.38	1154.68	7.3	0.15	0	42	58	60.9	51.6	36.5	-2.765	1101.93
1 min. after modification	4.3	1144.99	1144.99	1144.99	1153.92	8.92	0.27	0	29	71	72.2	105	45.5	-2.169	1098.42
7 min. after modification	4.3	1143.74	1143.74	1143.74	1153.32	9.58	0.32	0	27	73	78.7	76.1	38.8	-2.544	1101.67

Figure 4.5: ATAS thermal analysis data

4.2. 1^{st} Experiment results

All test castings were casted without any major surface defects. Castings were sanded, separated from gate system, two identical casting separated from each other and marked.

Casting session	C	Si	Mn	P	S	Cr	Mg	Cu	Sn	Al	Ni
1	3.7	2.31	0.28	0.035	0.01	0.039	0.053	0.028	0.007	0.006	0.014
2	3.79	2.41	0.33	0.038	0.015	0.043	0.06	0.034	0.005	0.005	0.016
3	3.69	2.39	0.33	0.035	0.011	0.041	0.073	0.035	0.004	0.005	0.015

Figure 4.6: Base metal composition for each casting session

Figure 4.7: Separated test casting (2 specimens) attached to runner

Casting session	t_1 [min:sec]	t_2	t_3	temperature at the end[°C]	Pouring time [sec]
1	6:30	t_1+56s	t_2+55s	1424	≈12
2	5:52	t_1+44s	t_2+75s	1410	
3	5:13	t_1+36s	t_2+40s	1417	

Figure 4.8: Time values during the experiment.

4.2.1. Shrinkage

In this section can be found results from density estimation and x-ray scanning. Full x-ray report can be found in appendix. X-ray scanning showed no porosity at all which was later confirmed by visual inspection after cutting test castings.

Specimen	Dry weight [g]	Water weight [g]	Immersed weight [g]	H20 weight [g]	Density [g/cm3]	Δρ [g/cm3]
11A	808.41	1169.39	1283.17	113.78	**7.105**	0.000
11B	794.29	1168.46	1280.26	111.8	**7.105**	
12A	817.24	1167.41	1283.6	116.19	**7.034**	-0.018
12B	823.54	1165.63	1282.42	116.79	**7.051**	
13A	807.82	1163.93	1277.74	113.81	**7.098**	0.078
13B	807.49	1162.74	1277.77	115.03	**7.020**	
21A	816.56	1160.76	1276.07	115.31	**7.081**	0.012
21B	806.78	1159.52	1273.65	114.13	**7.069**	
22A	789.16	1158.17	1269.28	111.11	**7.103**	0.006
22B	808.19	1157.17	1271.06	113.89	**7.096**	
23A	799.99	1156.04	1269.04	113	**7.080**	-0.018
23B	808.35	1154.96	1268.85	113.89	**7.098**	
31A	822.35	1153.94	1269.98	116.04	**7.087**	0.004
31B	810.11	1152.66	1267.04	114.38	**7.083**	
32A	815.89	1151.4	1265.8	114.4	**7.132**	0.003
32B	807.98	1150.31	1263.65	113.34	**7.129**	
33A	822.63	1149.34	1264.7	115.36	**7.131**	0.001
33B	814.91	1148.37	1262.67	114.3	**7.130**	

Figure 4.9: Results from double weightening density estimation

Specimen no.	Observable shrinkage	Type	Volume
11A	No	-	-
11B	No	-	-
12A	No	-	-
12B	No	-	-
13A	No	-	-
13B	No	-	-
21A	No	-	-
21B	No	-	-
22A	No	-	-
22B	No	-	-
23A	No	-	-
23B	No	-	-
31A	No	-	-
31B	No	-	-
32A	No	-	-
32B	No	-	-
33A	No	-	-
33B	No	-	-

Figure 4.10: Summary of observed shrinkage defects

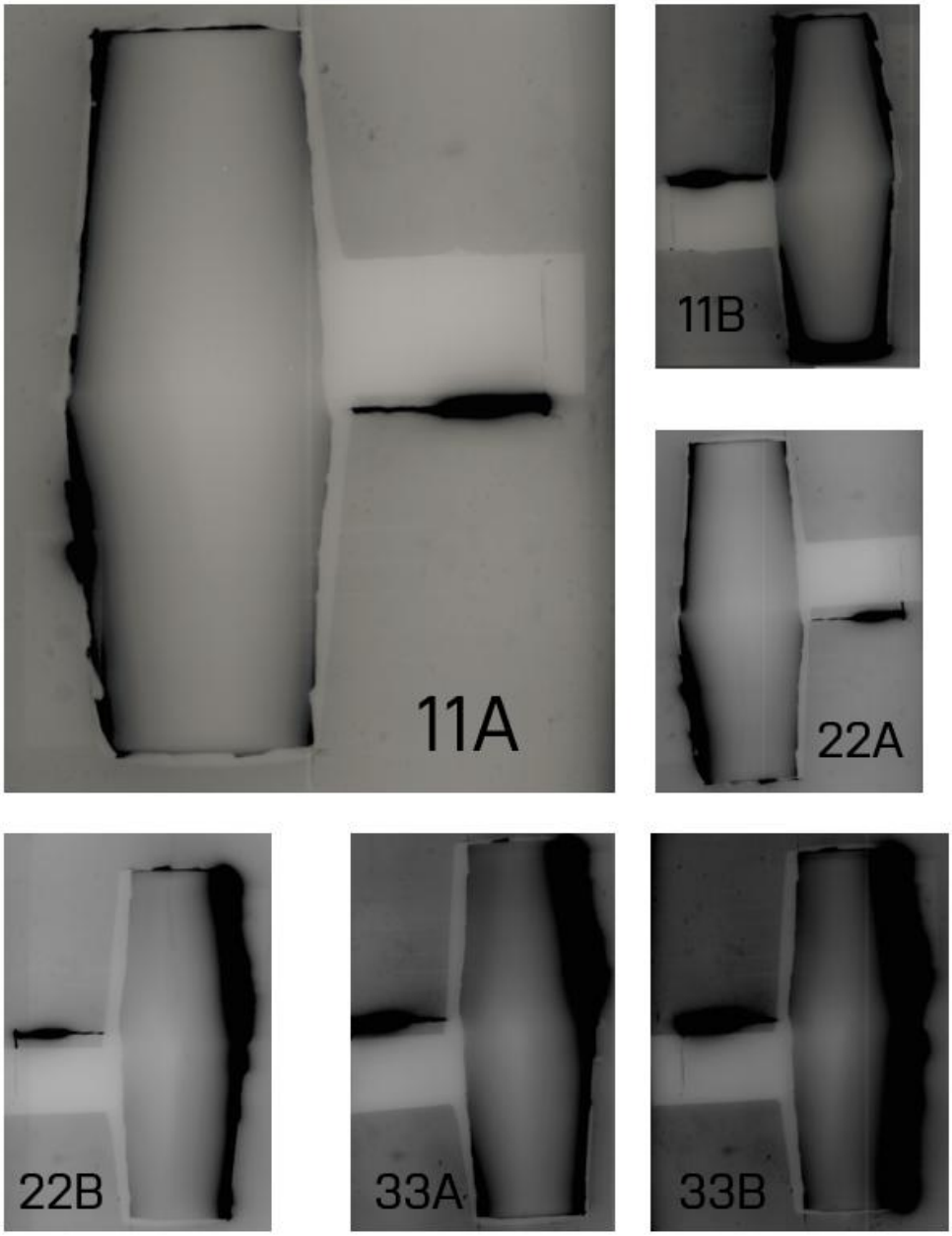

Figure 4.11: Example of x-ray images.

4.2.2. Microstructure

Microstructure evaluation was not done one every specimen. Evaluation was done from so from each inoculation amount and its matching thermal analysis sample is microstructure evaluation available.

Size of particles class	Size range [μm]	Sample no.					
		11	11T	12	12T	23	23T
4	120-240	3	-	2	-	-	-
5	60-120	2	2	3	-	4	-
6	30-60	28	12	34	34	22	12
7	15-30	151	103	91	100	125	94
8	<15	324	319	232	492	229	413
Sum of classes 4-7		**183**	**116**	**129**	**134**	**150**	**105**
Graphite Shape		Amount [%]					
III		2.7	2.6	17	15.6	5.3	6.6
V		41.5	22.4	73.6	41	36	33.3
VI		55.8	75	9.4	46.4	58.7	60.1
Structure		Amount [%]					
Pearlite		21	44	45	47	25	40

Figure 4.12: Evaluation of microstructure image analysis.

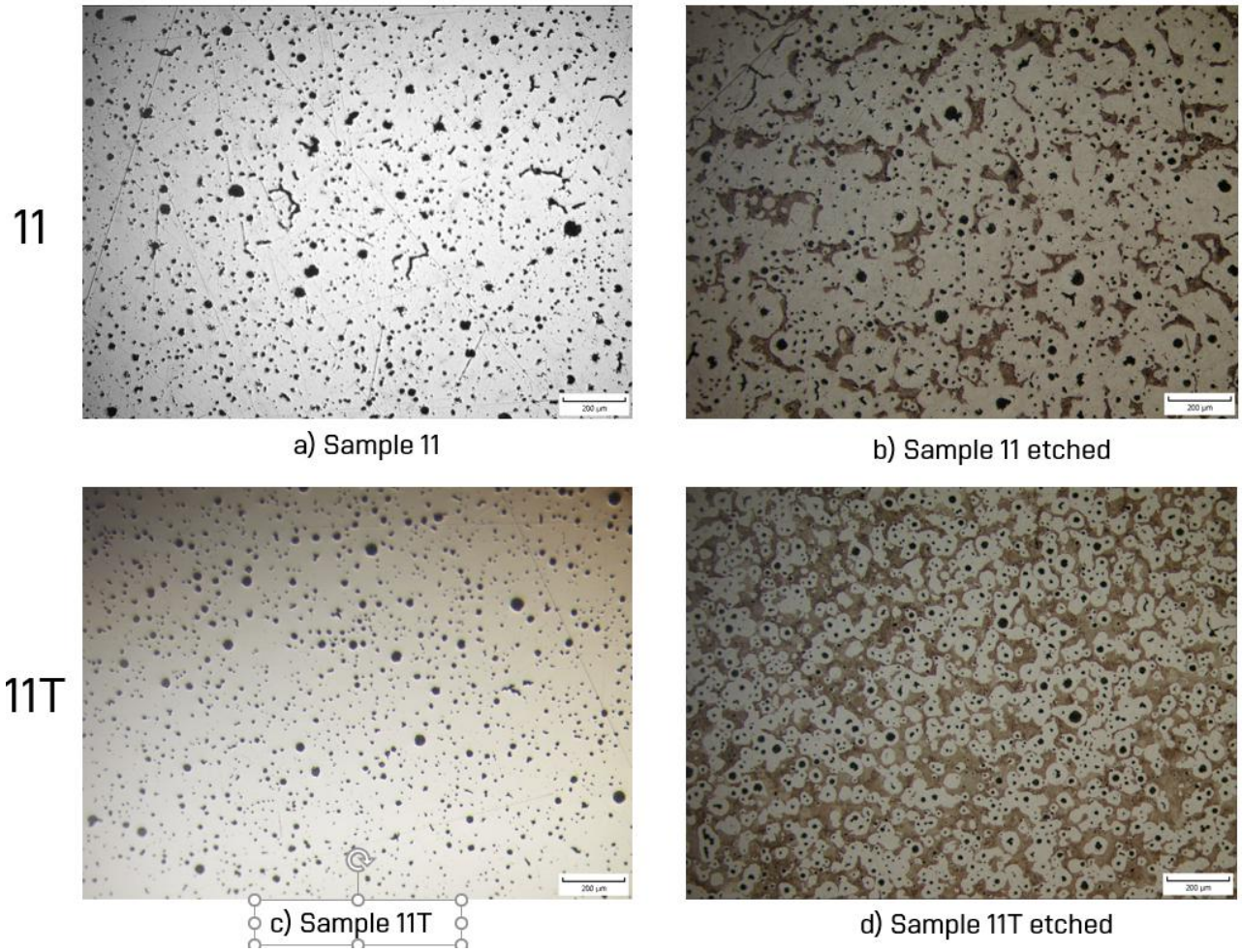

Figure 4.13: Images of sample 11 microstructure at 100x magnification.

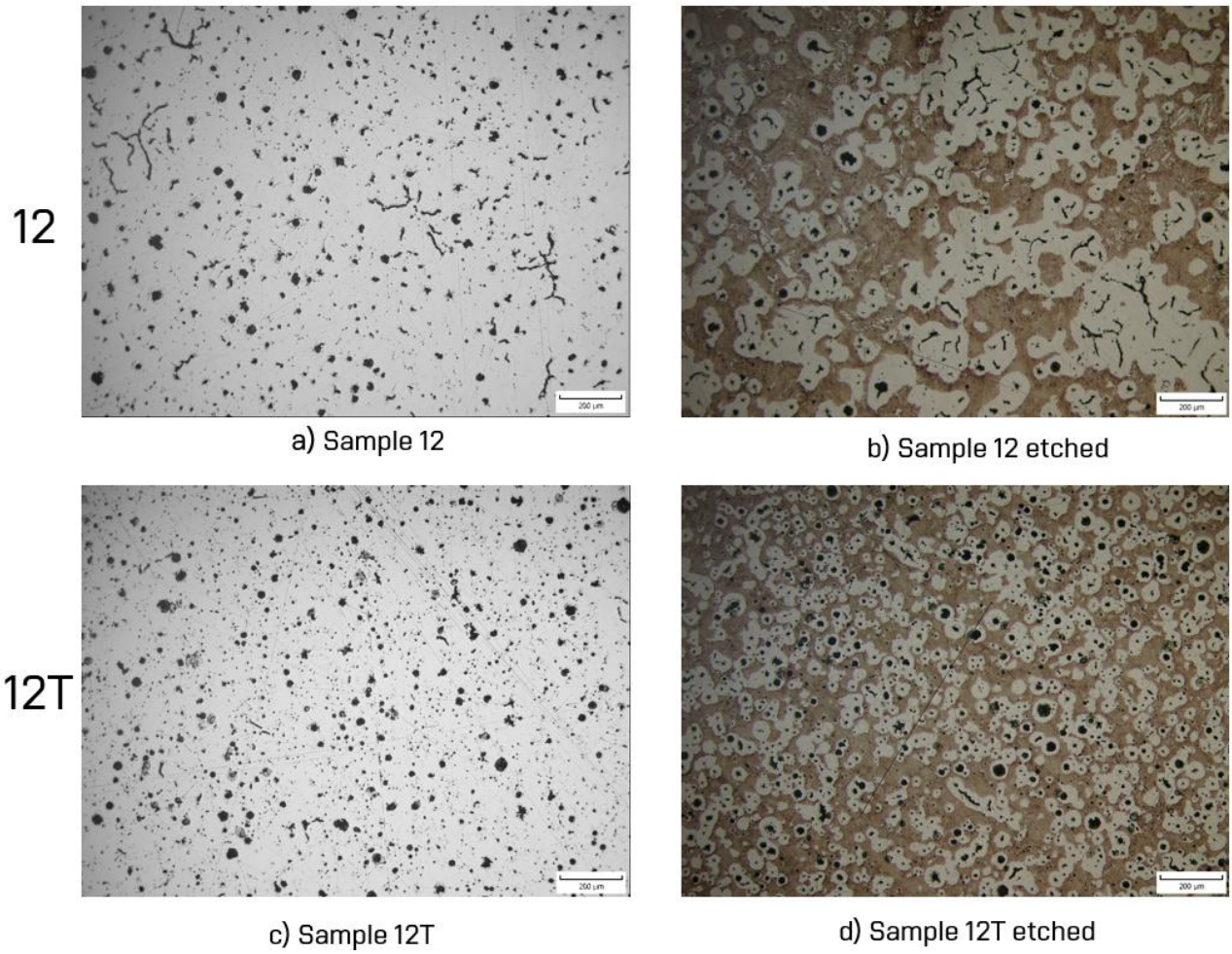

Figure 4.14: Images of sample 12 microstructure at 100x magnification.

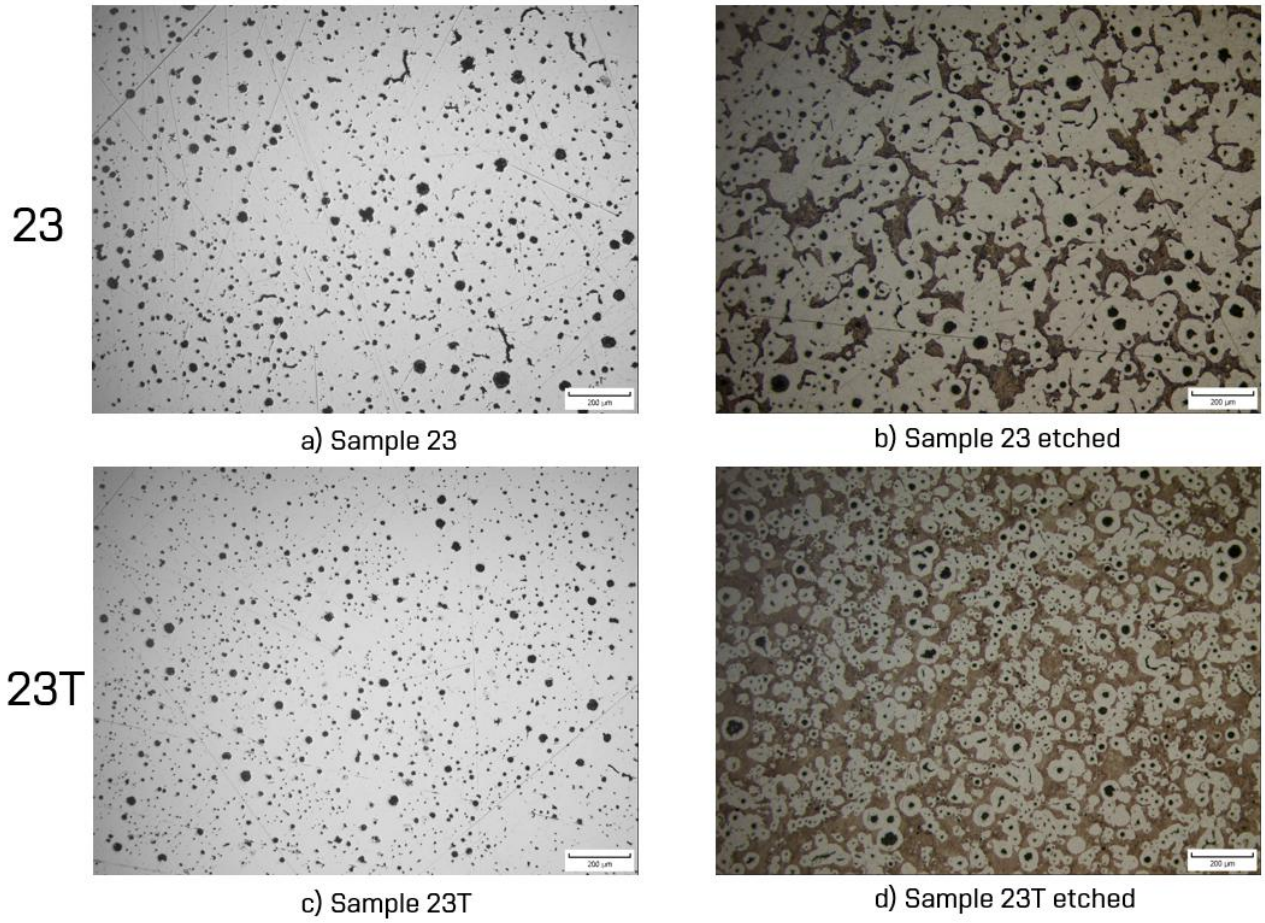

Figure 4.15: Images of sample 23 microstructure at 100x magnification.

4.2.3. Thermal analysis

Detailed ATAS thermal analysis data are included in appendix.

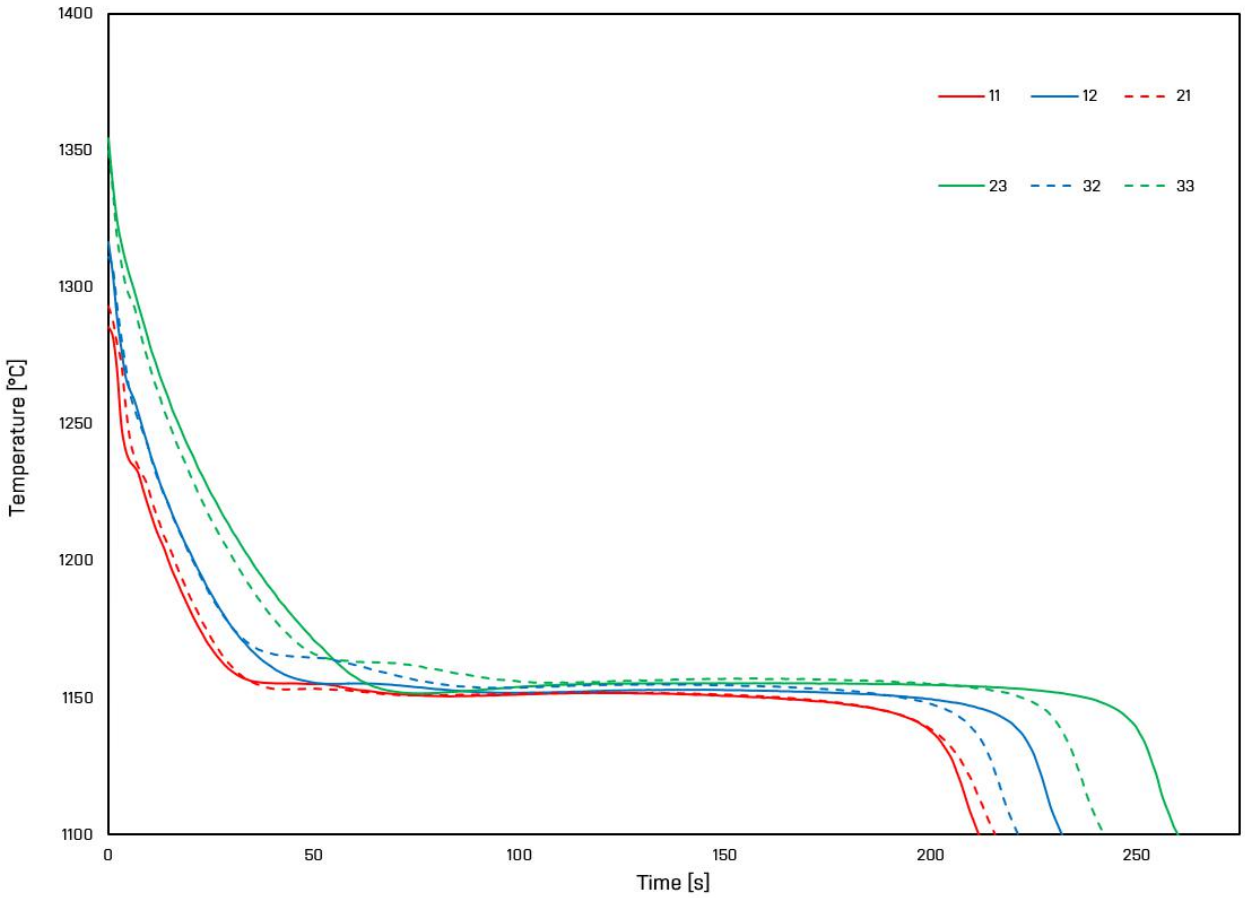

Figure 4.16: ATAS cooling curves from first experiment. Each color describes inoculation amount. Red - 2,4 g/s; Blue - 4,4 g/s; Green - 6,4 g/s

Specimen no.	ACEL	TL	dTdtTES	TES	TElow	TEhigh	R	MaxRrate	S1	S2	S3	GRF1	GRF2	GRF3	dTdtTS	TS
11	4.17	1155.1	-0.242	1153.61	1150.42	1151.62	1.19	0.05	24	22	54	84.9	27.6	31.4	-3.85	1110.41
12	4.17	1155.06	-0.144	1153.78	1151.72	1152.82	1.1	0.05	25	23	52	84.9	25.9	31.9	-3.96	1113.56
21	4.188	1153.02	-0.146	1151.88	1150.73	1151.65	0.92	0.04	20	26	54	78	40.7	34.5	-3.262	1107.93
23	4.3	1151.53	0	1151.53	1151.53	1155.2	3.67	0.12	0	40	60	73.3	25.7	28.3	-4	1116.38
32	4.084	1164.66	-0.384	1160.42	1153.52	1154.7	1.18	0.06	29	22	49	82.9	28.6	32	-3.805	1114.41
33	4.101	1162.76	-0.267	1159.45	1155.3	1156.83	1.53	0.05	26	27	47	75.6	28.1	29.6	-3.783	1118.53

Figure 4.17: ATAS thermal analysis data for first experiment.

4.3. 2^{nd} Experiment results

One test casting was casted containing three volumes (samples) with different in mold inoculation. Sample 44 had open shrinkage defect. Sample 41 had shifted thermocouple position. Pouring time was roughly 7 seconds.

Casting session	C	Si	Mn	P	S	Cr	Mg	Cu	Sn	Al	Ni
4	3.54	2.43	0.3	0.03	0.02	0.049	0.049	0.033	0.002	0.01	0.02

Figure 4.18: Base metal composition.

4.3.1. Shrinkage

Specimen	Dry weight [g]	H2O weight [g]	Density [g/cm3]
40	1783	252	7.075
41	1749	247	7.081
44	1767	252	7.012

Figure 4.19: Results from density estimation.

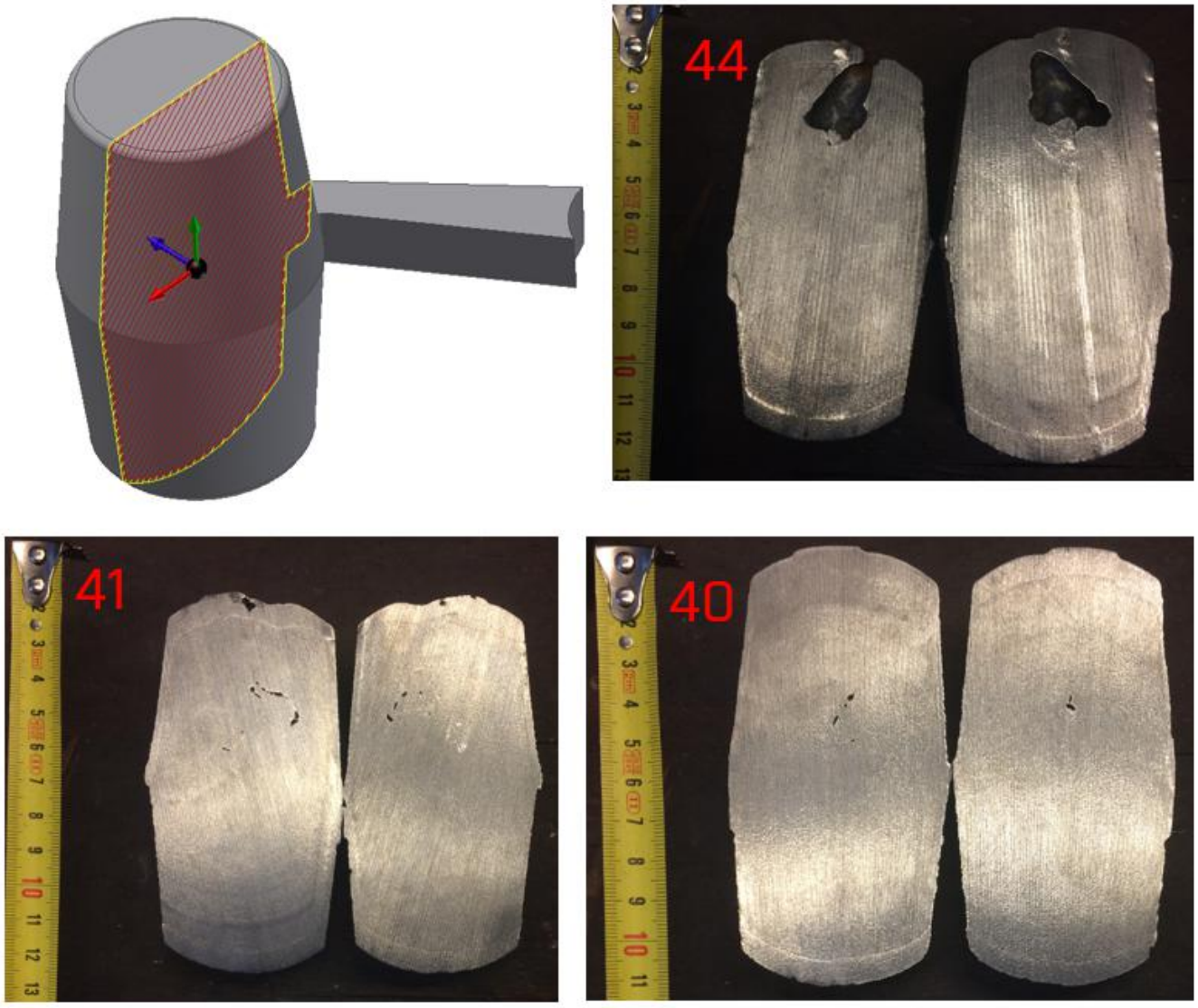

Figure 4.20: Sectioned specimens with shrinkage.

Specimen no.	Observable shrinkage	Type	Volume
40	Yes	Closed dispersed shrinkage	-
41	Yes	Closed dispersed shrinkage	-
44	Yes	Open macro shrinkage	2,2 cm^3

Figure 4.21: Summary of observed shrinkage defects.

4.3.2. Microstructure

Two microstructure measurements from single metalographic sample on two different places are taken. Values are summed and averaged.

Size of particles class	Size range [µm]	Sample no.					
		40	40	41	41	44	44
5	60-120	15	29	14	10	10	14
6	30-60	52	60	46	60	66	61
7	15-30	45	37	68	79	88	76
8	<15	36	9	19	17	22	21
Sum of classes 4-7		133	129	128	149	164	151
Average		131		138.5		149	
Graphite Shape		Amount [%]					
III		9.7	35.3	14.8	8.5	2.5	3.4
V		48	34.5	23.7	40.5	30.9	28.8
VI		42.3	30.2	61.5	51	66.6	67.8
Avg. III		22.5		11.7		3	
Avg. V		41.3		32.1		29.8	
Avg. VI		36.2		56.2		67.2	
Structure		Amount [%]					
Graphite		10,4		-		11	
Ferrite		60		66		68	

Figure 4.22: Evaluation of microstructure image analysis.

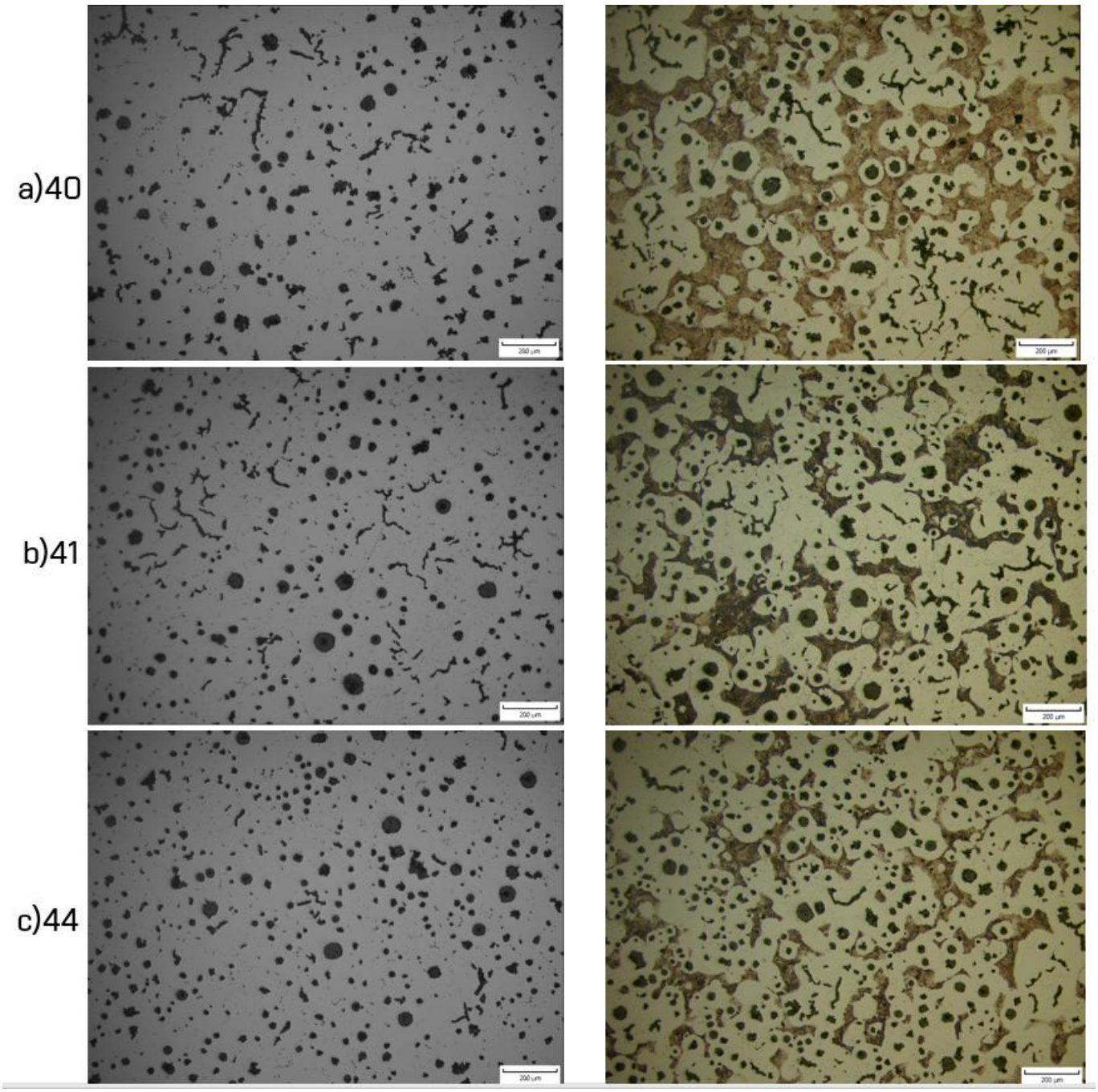

Figure 4.23: Images of samples 40, 41 and 44 at 100x magnification

4.3.3. Thermal analysis

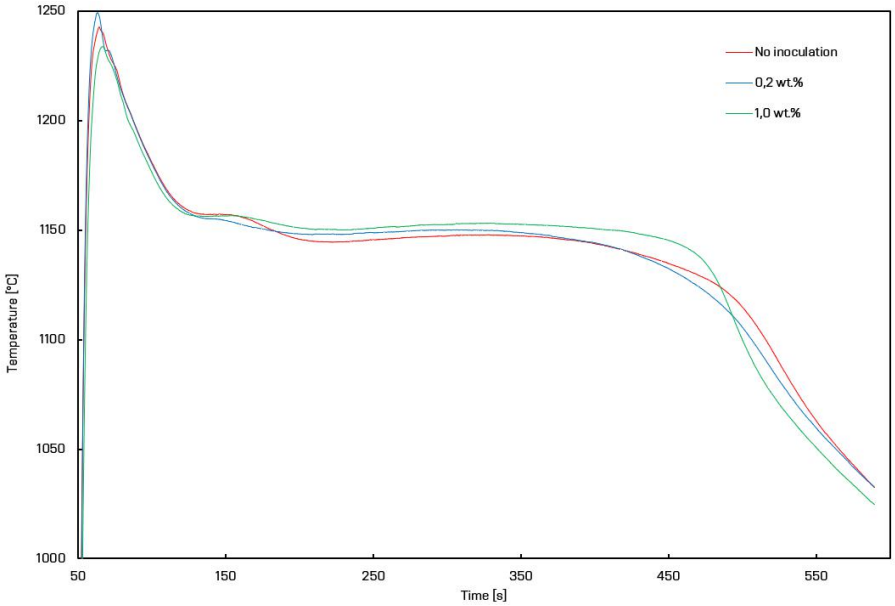

Figure 4.24: Cooling curves from thermo couples readings.

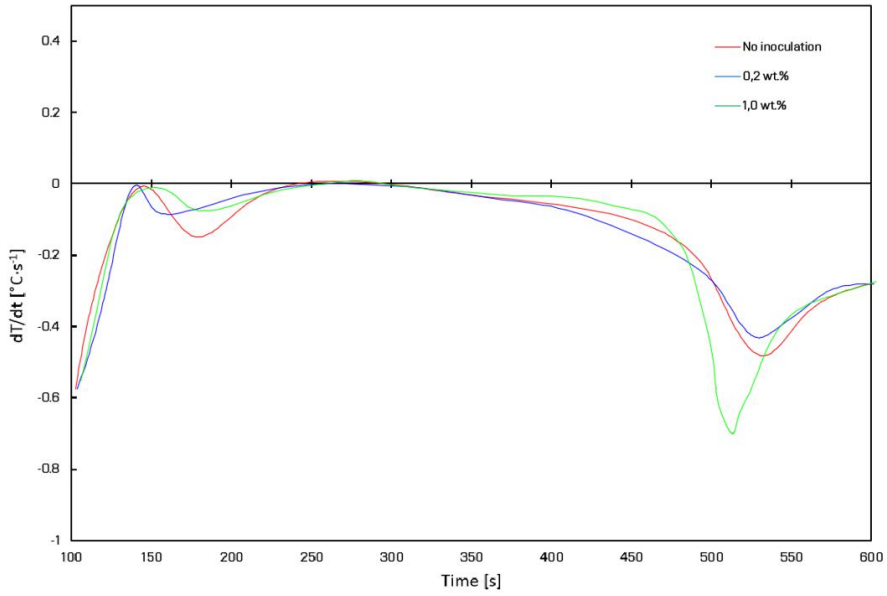

Figure 4.25: Cooling curves derivatives from thermo couples readings.

Specimen	ACEL	C	TL	dTdtTES	TES	TElow	TEhigh	R	MaxRrate	S1	S2	S3	GRF1	GRF2	GRF3	dTdtTS	TLplateau	TS
ATAS	4.136	3.521	1158.9	-0.246	1156.59	1153.13	1154.2	1.07	0.04	24	22	54	82.2	32.5	29.9	-3.514	30	1111.38
40			1157.1		1153.3	1144.5	1147.7	3.2						57.6		-0.47		1092.6
41			1155.3		1153.3	1148.1	1150	1.9						72.5		-0.41		1088.7
44			1156.1		1154.2	1150.2	1152.7	2.5						27.8		-0.65		1110.7

Figure 4.26: Cooling curves and derivatives thermal analysis estimated parameters compared with ATAS thermal analysis data.

5. Discussion

Preliminary tests showed that proposed design is reasonably sensible to shrinkage defects and produced various soundness of tested castings. This however, happen not to be true for following trials where different casting conditions played major role. Box type test casting was prone to surface sink as well as thermal analysis cup sample (Fig. 4.2). Surface sink defects can diminish presence of microporosity and this is not desirable behavior for this work. Cylinder castings showed no surface defects but amount of shrinkage defects happens to be corresponding to its box type counterpart castings. Cylinder test casting was chosen as a test casting for upcoming trials mainly.

First experiment unfortunately produced zero porosity defects in test casting which all were 100% sound. This was anticipated from density estimation (Fig. 4.9) where no substantial differences in density were found and confirmed with x-ray and visual observation. This outcome is probably due to different inoculation method and different inoculation used. Ladle inoculation happens to be less effective than in-stream inoculation because fading effect diminishes effect of inoculation over time whereas with in-stream inoculation there is no dwell time between pouring and inoculation. In addition Zircinoc inoculator is finer grade (Fig.3.0.3) hence dissolving in melt is easier. From this results can be concluded that method of inoculation and type of inoculator used have major impact on shrinkage defect presence and even low amounts of inoculation were sufficient with given conditions.

Microstructure evaluation of selected samples (Fig. 4.13, 4.14 and 4.15) did not revealed any relationship between inoculant amount and nodule count or any other evaluated parameters. This could mean that chosen range of inoculation rate have little to none impact for resulting quality. It is also apparent that sample and its matching thermal analysis sample does not match in terms of similarity. Reason for this could be different solidifying conditions for thermal analysis cup over production castings.

From this standpoint, conducted first experiment can not be considered as successful since no shrinkage defects were present hence no correlation with thermal analysis data can be done.

Experienced from first experiment, second one was done with test casting with enlarged volume to promote presence of shrinkage defects. As mold medium was chosen water glass to ensure even mold rigidity. Figure 4.26 ATAS data shows that base metal is of slightly hypo eutectic composition. Thermal couple in specimen 41 was shifted laterally by 8 mm accidentally however horizontal position remained unchanged, Figure **??** show that this shift had minimal if any observable impact on cooling curve.

In sample 44 was present open shrinkage, samples 40 and 41 suffered from small internal dispersed shrinkage (Fig. 4.20). Density evaluation was done with isolated open shrinkage so it was account into estimation (Fig. 4.19) which consequently resulted as slightly reduced apparent density. The fact that sample with most inoculation produced largest shrinkage defect is in contrary with common practice. This is because open shrinkage is formed at different stage than internal shrinkage. If origin of open cavity in sample 44 is of shrinkage nature, cavity was developed at early stage of solidification where solidified surface was not strong enough too prevent collapsing due to atmospheric pressure that is pushing against rising internal cavities that has much lower pressure inside. This lead to creation of open shrinkage lowering volume of casting greatly and diminishing potential for internal micro shrinkage creation. On the other hand, samples 40 and 41 have no open shrinkage defects and only graphite expansion was compensation for melts shrinking.

From microstructure images (Fig. 4.23) and its image analysis (Fig. 4.22) is clear that sample 40 and 41 have considerable amount of type III graphite. Effect of this can be seen in Figure 4.26 where estimated graphite factor 2 is much smaller for sample 44. This is expected since graphite factor 2 is indication for thermal conductivity at latest stage of solidification and smaller surface area of nodular graphite is affecting this greatly.

While thermal analysis parameters (Fig. 4.26) like temperature of solidification (TS) is raising with amount of inoculation which is expected, shrinkage occurrence is in contrary with common experience, no conclusion could be made since only one casting was made in second experiment, statistically it is not credible and more repetitions are required to be done. On the other hand, this setup showed to be good method to test inoculation

impact while keeping every other parameter literally same.

As for smoothing of cooling curves, ATAS data with density of one reading per second was not suitable for any further than first derivation. These data are processed inside ATAS software and provide wide rang of parameters. Cooling curve readings from second experiment using type S thermocouples have higher density of roughly 3 data reading per second, however generally speaking, at least 5 reading per second are needed for nice derivation. Second problem was that data reading scattering was relatively high as can be seen in Figure 3.5. In fact, data reading from termocoulples had higher spread than from ATAS making higher than first derivatives impossible. For this reason it was unable to determine position od dendrite coherency point for hypo-eutectic composition as Vitor [10] claimed that can be found in second derivative. For eutectic composition is dendrite coherency point determined at first minimum in first derivative which corresponds with start of eutectic freezing.

As can be seen, shrinkage porosity defects in cast irons have very complex nature of origin and considerable amount of variables like pouring temperature, mold rigidity, chemical composition, type and method of inoculation, number of potential nucleation sites for shrinkage pores, casting geometry, feeding conditions and more have impact on final shrinkage occurrence. This is making testing and experiment complicated to really distinguish impact of single variable on shrinkage defects. Testing in foundry had its limitations, for example it was not possible to purposely prepare malt of bad quality to promote shrinkage for economic reasons. Position of thermal analysis stand was not optimal for this experimentation since thermal analysis cups were used rather after tapping the metal then just before casting. Inability to effectively "simulate" real melt composition which is inoculated into stream making thermal for analysis for predicting shrinkage not ideal conditions. Idea was to keep basic melt composition and more importantly eutectic during whole experimentation since solidification of eutectic and hypo-eutectic is slightly different however, this was not the case.

With obtained experience I'm suggesting few ideas for further experimentation to follow up with results in this work.

- Experiment should be independent from restricting foundry process and make preparation of melt and casting conditions more flexible.
- Have thermal analysis stand next to pouring field and test only melt only in its final condition just before casting.
- Test both resin bonded and green sand molds.
- Test different inoculant types in different amounts within one melt session.
- Produce larger amount of samples to make data more robust.
- Different thermal analysis cup geometry should be considered. AccuVo-Cup from OCC would be much better choice.

6. Conclusion

In this work, two experiments were done to obtain cooling curves from casting and thermal analysis data to study them and find correlation between parameters from thermal analysis and shrinkage defects present in test castings. First experiment was done on automated molding link with test casting attached to gating system of production casting. With given set of conditions and parameters. No porosity was observed in any of test castings therefore gained data couldn't been correlated with shrinkage making this experiment unsuccessful. Second experiment narrowed down changing parameters to single one, which was inoculation amount. This produces shrinkage however of different types that could not be directly compared. In addition only one casting was casted hence results from second experiment have zero significance. This made second experiment data limited for making deeper and more complex conclusions. Discussion summarized and commented on obtained data and experience with proposed solutions and recommendations for further testing.

Bibliography

[1] ROUCKA, Jaromír: & Brno university of technology (2018): *Metalurgie litin*

[2] STEFANESCU, D. M.: *Clasification and Basic Meallurgy of Cast Iron.* The University of Alabama, 1990., 3-11. 10.1361

[3] STEFANESCU, D. M.: *Thermal AnalysisTheory and Applications in Metalcasting.* International Journal of Metalcasting, 9. 7-22.

[4] STEFANESCU, D. M.: *Science and Engineering of Casting solidification.* The Ohio State University, 2009, ISBN 978-0-387-74609-8

[5] CAMPBELL, J.: *Castings.* ISBN 0 7506 4790 6

[6] SILLEN, R.: *Production of Ductile Iron Castings without Feeders.*, 2007, NovaCast Technologies, Sweden

[7] KANNO, T. et al.: *Prediction of Graphite Nodule Count and Shrinkage Tendency of Spheroidal Graphite Cast Iron by One Cup Thermal Analysis.*, 2018,Materials Transactions, 59.

[8] SINGH K. K. & Sethy S. K.: *Recalescence and shrinkage relationship in ductile iron: study on front engine support casting by thermal analysis.* International Journal of Cast Metals Research, 26:3, 168-175

[9] BOCKUS, S. et al.: *The Impact of Volume Shrinkage of Ductile Iron on The Feeder Size.* Metal 2005

[10] EMANUEL, V.: *Use of Thermal Analysis to Control the Solidification Morphology of Nodular Cast Irons and Reduce Feeding Needs.*

[11] BRADLEY, F. & Fung, C.A.: *Thermal analysis for shrinkage prediction in commercial ductile iron castings.*, 1991

[12] NovaCAST: *ATAS User Guide*

[13] Heraeus Group: *Thermal Analysis of Cast Iron*, https://*www.heraeus.com/*

[14] Quantitative Decisions: *Smoothing*, *http* : *//www.quantdec.com/Excel/smoothing.htm*